AEDC-TR-75-65

[redacted]

Unclassified

EXPERIMENTAL STUDY OF THE REAL GAS EFFECTS OF NITROGEN AND AIR TO 3000 ATMOSPHERES AND 3500 K

VON KÁRMÁN INSTITUTE FOR FLUID DYNAMICS
72 CHAUSÉE DE WATERLOO
1640 RHODE-ST-GENÈSE, BELGIUM

July 1975

Final Report for Period September 1, 1973 — August 31, 1974

Approved for public release; distribution unlimited.

[redacted]

Prepared for

ARNOLD ENGINEERING DEVELOPMENT CENTER (DY)
AIR FORCE SYSTEMS COMMAND
ARNOLD AIR FORCE STATION, TENNESSEE 37389

Unclassified

NOTICES

When U. S. Government drawings specifications, or other data are used for any purpose other than a definitely related Government procurement operation, the Government thereby incurs no responsibility nor any obligation whatsoever, and the fact that the Government may have formulated, furnished, or in any way supplied the said drawings, specifications, or other data, is not to be regarded by implication or otherwise, or in any manner licensing the holder or any other person or corporation, or conveying any rights or permission to manufacture, use, or sell any patented invention that may in any way be related thereto.

Qualified users may obtain copies of this report from the Defense Documentation Center.

References to named commercial products in this report are not to be considered in any sense as an endorsement of the product by the United States Air Force or the Government.

This final report was submitted by von Kármán Institute for Fluid Dynamics, 72 Chaussée de Waterloo, 1640 Rhode-St-Genèse, Belgium, under contract AFOSR-72-2413, with the Arnold Engineering Development Center (AEDC), Arnold Air Force Station, Tennessee 37389. Mr. Elton R. Thompson, DYR, was the AEDC Project Scientist.

This report has been reviewed by the Information Office (OI) and is releasable to the National Technical Information Service (NTIS). At NTIS, it will be available to the general public, including foreign nations.

APPROVAL STATEMENT

This technical report has been reviewed and is approved for publication.

FOR THE COMMANDER

Elton R. Thompson

ELTON R. THOMPSON
Research & Development
Division
Directorate of Technology

Robert O. Dietz

ROBERT O. DIETZ
Director of Technology

REPORT DOCUMENTATION PAGE

READ INSTRUCTIONS BEFORE COMPLETING FORM

1. REPORT NUMBER: AEDC-TR-75-65

2. GOVT ACCESSION NO.

3. RECIPIENT'S CATALOG NUMBER

4. TITLE (and Subtitle): EXPERIMENTAL STUDY OF THE REAL GAS EFFECTS OF NITROGEN AND AIR TO 3000 ATMOSPHERES AND 3500 K

5. TYPE OF REPORT & PERIOD COVERED: Final Report - 1 Sept 1973 - 31 Aug 1974

6. PERFORMING ORG. REPORT NUMBER

7. AUTHOR(s): Georges P. Rouel and Bryan E. Richards

8. CONTRACT OR GRANT NUMBER(s): AFOSR-72-2413

9. PERFORMING ORGANIZATION NAME AND ADDRESS: von Kármán Institute for Fluid Dynamics, 72 Chaussée de Waterloo, 1640 Rhode-St-Genèse, Belgium

10. PROGRAM ELEMENT, PROJECT, TASK AREA & WORK UNIT NUMBERS: Program Element 65802F, Projects T-1(YA) and T-2(YB)

11. CONTROLLING OFFICE NAME AND ADDRESS: Arnold Engineering Development Center(DYFS), Air Force Systems Command, Arnold Air Force Station, Tennessee 37389

12. REPORT DATE: July 1975

13. NUMBER OF PAGES: 61

14. MONITORING AGENCY NAME & ADDRESS (if different from Controlling Office)

15. SECURITY CLASS. (of this report): UNCLASSIFIED

15a. DECLASSIFICATION/DOWNGRADING SCHEDULE: N/A

16. DISTRIBUTION STATEMENT (of this Report)

Approved for public release; distribution unlimited.

17. DISTRIBUTION STATEMENT (of the abstract entered in Block 20, if different from Report)

18. SUPPLEMENTARY NOTES

Available in DDC

19. KEY WORDS (Continue on reverse side if necessary and identify by block number)

thermodynamics	temperature	research facilities
gases	volume	
nitrogen	high density	
air	high temperature	
pressure	reentry vehicles	

20. ABSTRACT (Continue on reverse side if necessary and identify by block number)

A free piston compression tube has been used to generate samples of nitrogen and air test gases at pressures up to 3000 kg/cm^2 and 3500 K. Measurement of pressure, temperature and volume during part of the cycle has been made. The experiments utilize piezoelectric transducers, a sodium line reversal technique and an eddy-current transducer. Calculations and experiments have been carried out which have indicated that the level of uncertainty of measurement of these parameters is below ±5% at peak conditions and within

DD FORM 1 JAN 73 1473 EDITION OF 1 NOV 65 IS OBSOLETE

20. ABSTRACT (Continued)

±10% at conditions away from the peak. The main emphasis in this phase of a continuing research program is on the generation of data in nitrogen and air over the widest range possible in the facility. Regions in the Mollier chart in which measurements become more uncertain are specified. Extensive analysis of the data has illustrated that larger differences between experiment and equation of state models have been found than earlier results indicated. Correlations, however, give strong indications that the models, and the pressure and density measurements are accurate, and the nitrogen and air gas sample generated is relatively homogeneous and contamination free. The main error appears to occur in the temperature measurement and it is suggested that the sodium line reversal method is strongly affected by even small quantities of contamination. Other interpretations of the differences seen are also discussed.

AFSC
Arnold AFS Tenn

PREFACE

The work reported was sponsored by the Arnold Engineering Development Center (AEDC), Directorate of Technology, under Projects T-1(YA) and T-2(YB), Program Element 65802F with Mr. Elton R. Thompson acting as Project Scientist. The report covers work conducted during the period September 1st 1973 to August 31st 1974.

The authors, Georges P. Rouel and Bryan E. Richards, are grateful to Dr. L. Bernstein of Queen Mary College, London, for the loan of equipment used in the sodium line reversal system for measuring temperature.

The assistance of the technical engineers Roger Conniasselle and Roger Borrès and that of Fernand Vanden Broeck was greatly appreciated. The manuscript was typed by Mrs. L. Rigaux.

The reproducibles used in the reproduction of this report were supplied by the authors.

TABLE OF CONTENTS

LIST OF ILLUSTRATIONS

LIST OF TABLES

INTRODUCTION

Aerodynamic ground test facilities for simulating re-entry flows involve the use of very high operating pressures at high temperatures (Ref.1). Under these conditions the equation of state departs markedly from the perfect gas law due to compressibility effects and excitation of internal energy modes. The associated thermodynamic properties are hence also strongly influenced. Optimisation studies of ground test facilities require that such gas imperfections are known with a reasonable degree of accuracy. This report describes an experimental program to make accurate measurements of pressure, volume and temperature of nitrogen and air at pressures up to 3000 atmospheres and temperatures up to 3500 K, a range of conditions in which the compressibility effects are most dominant.

The behaviour of dense gases may, in principle, be predicted using quantum-statistical mechanics. However, the mathematical difficulties involved when molecular interactions must be taken into account are so formidable that solutions have only been found using highly simplified molecular models (Ref.2). Many attempts have been made to obtain semi-empirical equations of state which are valid for any dense gas by the application of Van der Waals' principle of corresponding states (Refs. 3 and 4). These depend on having available knowledge of the equations of state over the range required. Once the equation of state is defined, all thermodynamic properties can be obtained from existing relations (Ref.4).

Up to present experiments, providing the knowledge on which the equations of state are based, have been confined to the studies of gases at high pressures and ordinary temperatures, where measurements may be made under steady state conditions. A large amount of data is available in this regime. The contrary is true at high temperatures because of the problems encountered in maintaining the structural integrity of the containing vessel. These problems can be overcome by rapidly heating and compressing a gas sample by a piston, and taking the desired measurements under transient conditions.

The driver section of the VKI Piston Driven Shock Tube has been modified to generate samples of dense high temperature gases and instrumentation has been developed to measure pressure, temperature and density (Refs. 5, 6). A sodium spectral line reversal technique is used to measure the temperature of the gas. The density of the gas is determined indirectly by measuring the piston's position during the compression process. This measurement involves the use of an eddy current displacement transducer. A quartz-crystal piezo electric transducer is used to measure the pressure of the gas. More details of the instrumentation are given within and in Ref.6.

The report describes experiments carried out to generate thermodynamic state data of nitrogen and air for an extended range of conditions than reported in Ref.6. Particular attention is paid to new observations and new techniques developed recently. The results for nitrogen are then compared with the Enkenhus and Culotta (Ref.4) equation of state model which agrees accurately with the tables

generated by Grabau and Brahinsky (Ref.7) and the results for air are compared with the tables generated by Grabau and Brahinsky (Ref.8). These latter tables were developed at AEDC.

2. EXPERIMENTAL TECHNIQUE

2.1 The test gas compression system

The system for compressing the gas is illustrated in Fig.1. A piston constructed of hardened steel, aluminium and nylon, weighing 12.6 kg and of length 250 mm is free to move in a barrel of 92.8 mm diameter and 1.98 m in length. The barrel is attached to a reservoir, of diameter 270 mm and length 2.3 m at one end and is closed at the other end. Initially an aluminium diaphragm, typically of thickness 0.4 mm, retains the piston at the reservoir end of the barrel. The gas under test is introduced into the barrel, after evacuating and purging the barrel with the use of a vacuum pump, and the reservoir is charged with air up to its operating pressure P_0 at temperature T_0. The piston is released and driven down the barrel compressing the test gas from an initial pressure P_{4_i} and T_{4_i} to a maximum pressure P_{4_f} and temperature T_{4_f}. Both T_0 and T_{4_i} are equal to the laboratory temperature. The piston is instantaneously at rest when the peak pressure is achieved. After the first compression stroke, the piston reverses its motion and returns to the reservoir end of the barrel. It continues to oscillate in the barrel until brought to rest by friction. Values of P_{4_f} up to 3000 kg/cm^2 can be achieved depending on the initial pressure ratio across the piston. This limitation is imposed by the strength of the barrel and its end fittings.

The pressure (P_4), temperature (T_4) and density (ρ_4) variations of the nitrogen are measured during the first compression stroke. Typically, the initial barrel pressure measured by means of either a mercury manometer or

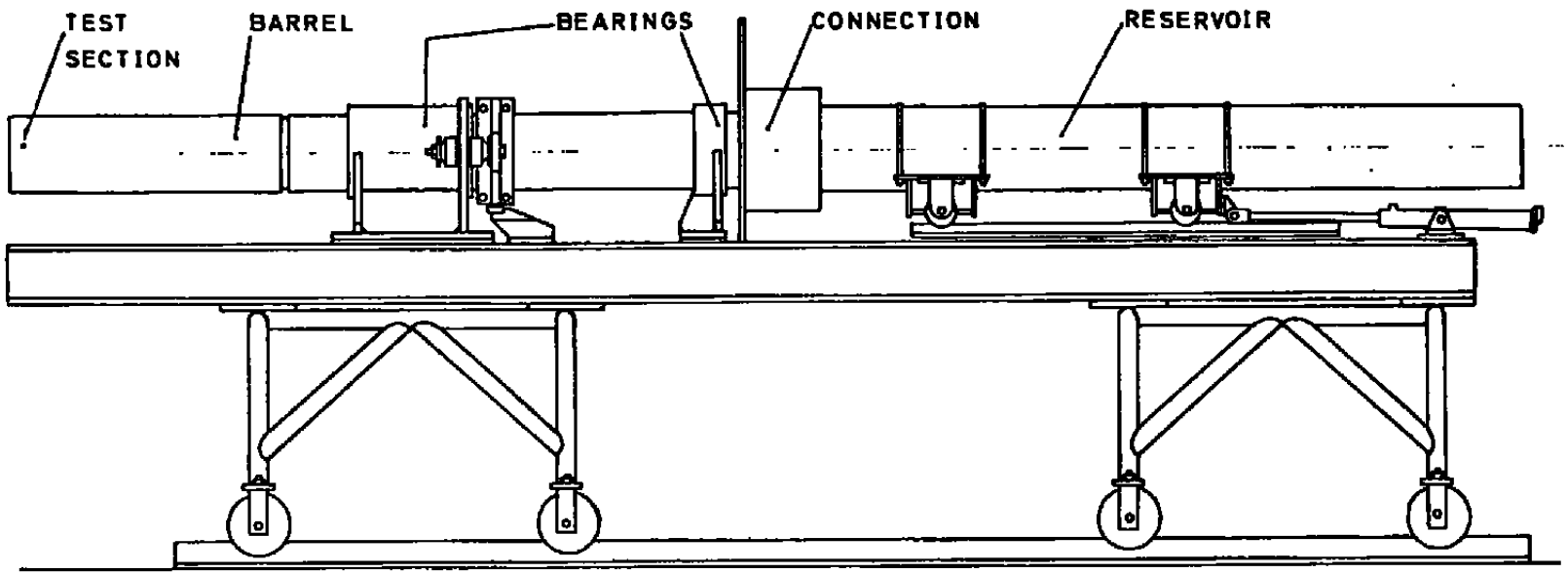

FIG. 1 - General assembly of compressor

a Wallace and Tiernan gauge is between 0.1 to 10 kg/cm^2; the transit time of the piston from its initial rest position to its "peak pressure" rest position is about 50 msec. The total measurement time of interest is of the order of 1 msec. During this time, the piston is between 10 and 40 mm from the closed end of the barrel.

2.2 Pressure instrumentation

The pressure variation of the test gas during the stroke is measured using either a Type 6221 or Type 6201 Kistler piezo-electric pressure transducer and a Kistler 568/M5 charge amplifier and recorded on a Tektronix Type 502A Oscilloscope. The transducer is mounted in the wall and near the end of the barrel, as depicted in Fig.2. The oscilloscope trace is photographed with a Polaroid camera. The calibration and assessment of accuracy of the pressure measuring system is described in Ref.6.

2.3 Temperature instrumentation

The temperature of the test gas is determined by using the sodium-line reversal technique (Ref.9) illustrated in Fig.3. A single source effective double beam system, described in full in Refs. 5 and 6, is used.

In the early tests, a Philips D-8, 6 volt, 16-17 amp rated tungsten ribbon lamp is used as a background light source for the sodium line reversal technique. The maximum temperature achieved by this source is approximately 2300 K.

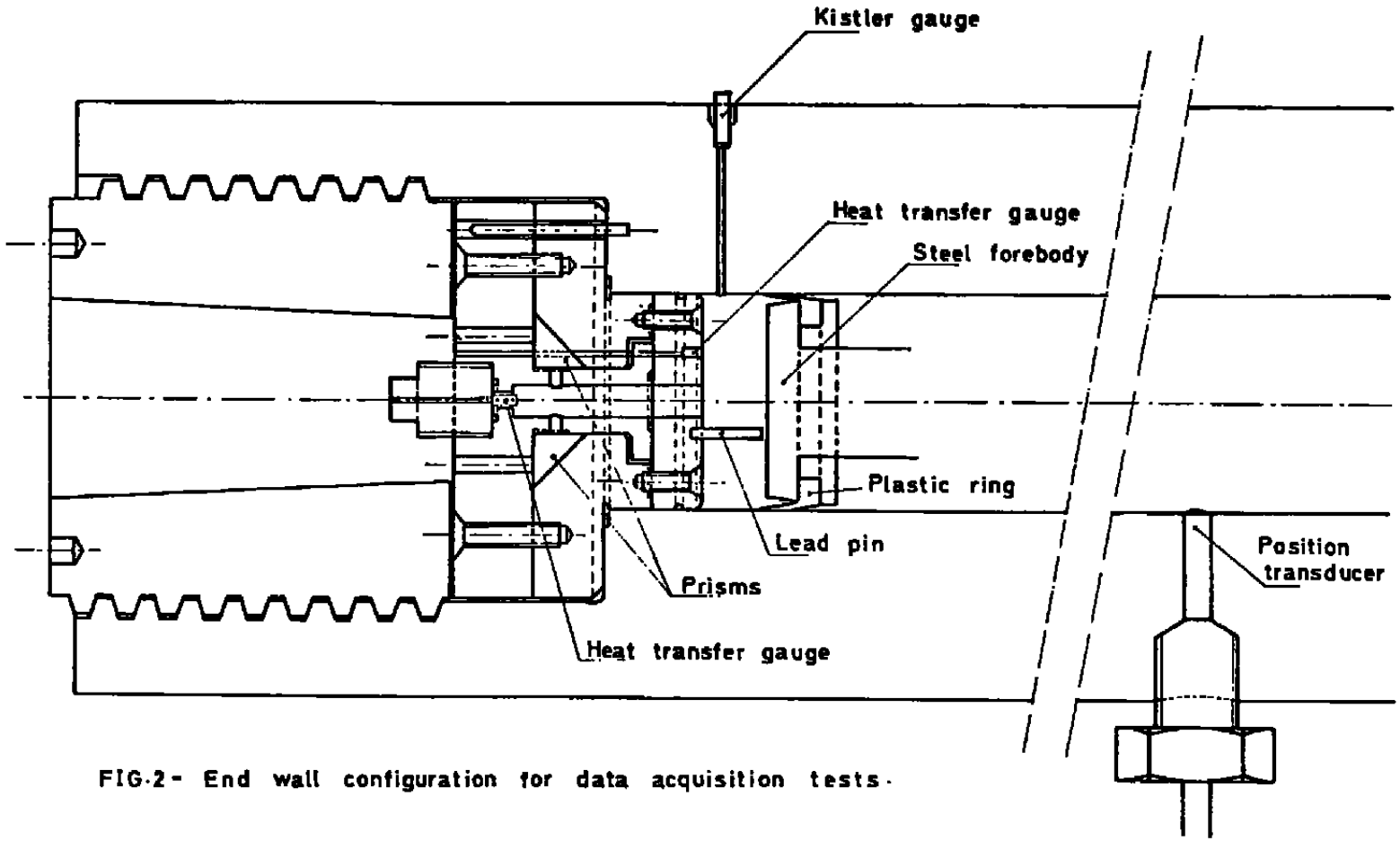

FIG.2- End wall configuration for data acquisition tests.

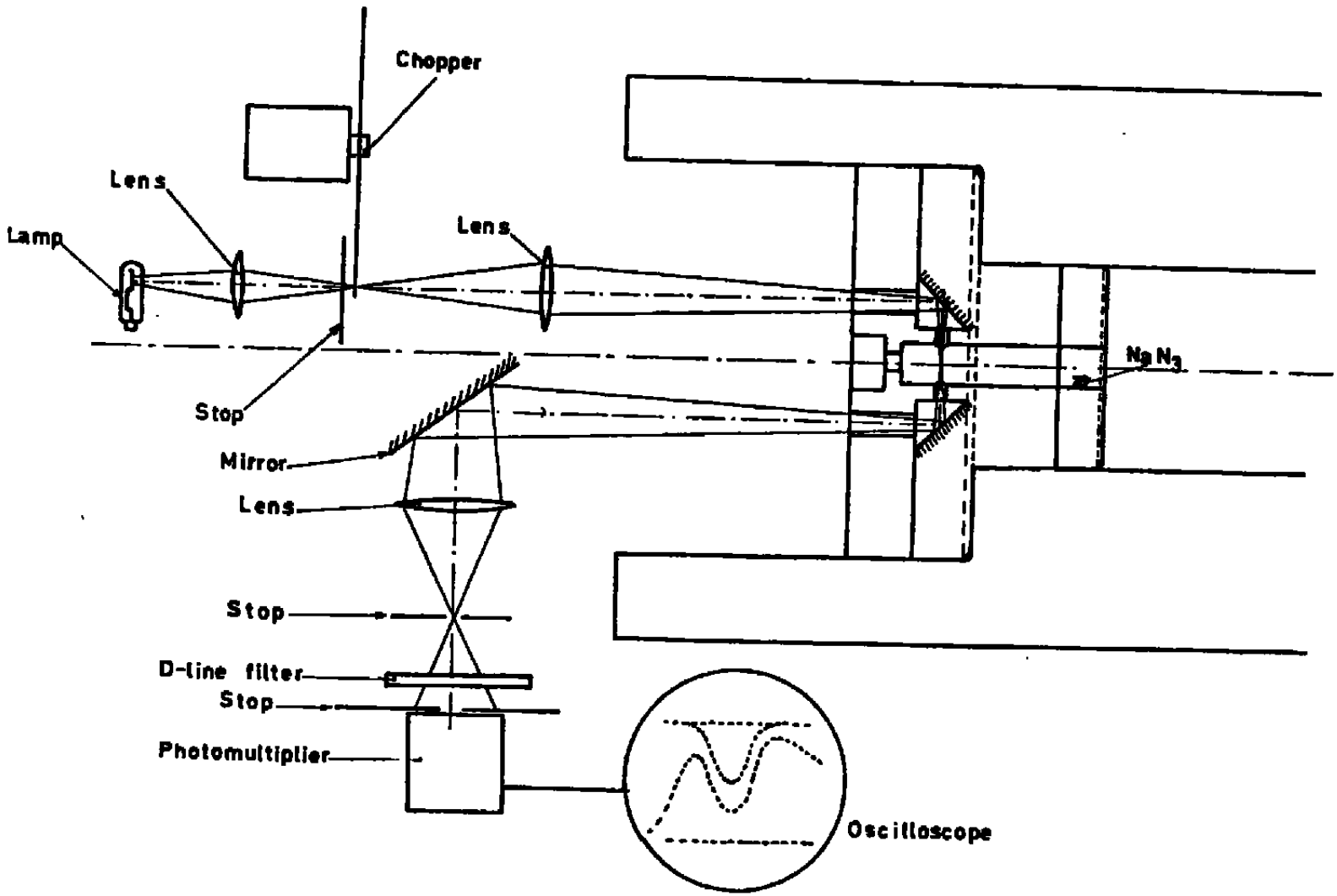

FIG. 3 - Sodium line reversal system

In order to extend the range of the experiments to 3500 K, a Spindler and Hoyer Carbon Arc Source was acquired and used instead of the tungsten ribbon source. The Carbon Arc Source provides a non-varying standard temperature of 3800 K. The light is emitted from a crater in the positive electrode caused by the phase change from solid carbon to gas in turn caused by the arc across the electrodes. The emissivity of the centre of the crater is assumed to be that of a black body and equal to 1. A detailed discussion of such a light source is given in Refs. 10 and 11. The temperature of the source can only be altered by applying neutral filters between the source and the test section.

The Spindler and Hoyer lamp is powered by the Institute's 220 V DC supply which has a very small residual ripple. A resistor of 27.5 ohms is placed in series with the source to supply it with its rated 55 V and 6 amps across the electrodes. The positive carbon electrode (6 mm diameter by 200 mm length type NORIS homogeneous) is positioned horizontally. The negative carbon electrode (7 mm diameter by 125 mm length, type NORIS homogeneous) is positioned vertically at a distance from the positive electrode varying between 2-5 mm. The voltage across the anode and cathode during operation varies with distance between them. In order to allow continuous operation then an electric motor is fitted to feed the electrodes into their correct position as they are burnt. The rate of feed is controlled by means of keeping the voltage across the electrodes to within pre-determined limits. Because of the method used the feed of electrodes is not smooth. Two other sources of uncertainty were examined. Firstly the 27.5 ohm resistor becomes heated due to the high current passing through it,

causing resistance and hence supply voltage changes. This effect is, however, compensated by the continuous feed system. Secondly the displacement of the positive electrode by several millimeters during feeding causes a tendency to place the system in an unfocussed condition.

The performance of the carbon arc and the optical system was examined using an Evershed and Vignoles optical pyrometer in a similar manner to that described in Ref.6. When focussed directly on the crater of the positive electrode, the optical pyrometer gave a temperature of 3770 K with a reading scatter of ±40 K. This scatter is attributed to subjectivity errors in reading the pyrometer, and to the uncertainties caused by the variation of the gap size between the electrodes. This calibrated value compares well with the expected temperature of a carbon arc source detailed in Ref.10 of 3800 K.

The temperature measured at the test section position after the light had passed through the measuring system optics was 3460 K, with a similar scatter as before. Although some optically flat glass slabs were tested for their application as neutral filters to vary the background temperature to the SLR system, these, however, were not used. It was found that the source could be used to provide an adequately large range of conditions below 3500 K without such filters.

The overall uncertainty of the system with the carbon arc background source was assessed to be ±1.5%, i.e. similar to that incurred using the tungsten ribbon background source at low temperatures (Ref.6).

2.4 Density measurement

The density variation of the compressed nitrogen is determined from accurate measurements of the piston's position relative to the barrel during the final stages of the compression stroke.

Two complementary systems are used. A small lead pin, mounted in the end wall of the barrel, is crushed by the piston. The length of the crushed pin gives the displacement L of the piston from the end wall at peak pressure. Away from peak pressure, the piston's position is monitored at intervals of one millimeter by a displacement transducer mounted in the side of the barrel. The pin and transducer positions are shown in Fig.2. The latter's position prevents the transducer from being subjected to pressure levels above 30 kg/cm^2. The transducer, a commercially available Vibrometer TW6-100/A eddy-current contactless displacement transducer, monitors accurately machined grooves on an aluminium sleeve attached to the piston. The transducer is excited by a Vibrometer type 100 TRI/A carrier amplifier.

Knowing the piston position relative to the transducer, the displacement (L) and volume (V_4) of the compressed gas may be determined from the geometry of the barrel and piston. The number of moles M, of gas in this volume is known from a measurement of the initial volume V_{4_i}, pressure P_{4_i}, and temperature T_{4_i}. The density of the gas is given by

$$\rho_4 = \frac{M}{V_4}$$

$$\rho_4 = \frac{P_{4_i} V_{4_i}}{RT_{4_i} V_4} \qquad (1)$$

where R is the gas constant per mole. In deriving Eq.1, it is assumed that no gas leaks past the piston during the compression stroke.

An assessment of the uncertainty of the measurement of density is given in Ref.6.

2.5 Compression cycle measurement control system

During the final stages of the piston compression stroke, the pressure, temperature and piston position signals are recorded simultaneously. The output from the position transducer triggers the sweep of the oscilloscopes. The vertical amplifier of the Tektronix Type 531A oscilloscope used to record the position measurement operates in the DC mode and is adjusted so that a signal is recorded only when the grooves on the piston are traversing the transducer. The time scale of the trace is extended by using the four alternate trace capability of the oscilloscope's type M plug-in unit. A four trace "raster" display, which has a calibrated sweep-back time of 30μsec, is obtained. The oscilloscope monitoring pressure and temperature signals operates in the single-sweep mode to prevent recording compression strokes other than the first. Base lines on the traces are added just before each test. To correlate the time scales of the two oscilloscopes, a one-kHz square wave of small amplitude is superimposed upon the pressure measurement and piston

position measurement signals.

2.6 Summary of measurement uncertainties

The following table summarises the results of the uncertainty study of the measurements at peak conditions for which detailed discussion is given in Ref.6.

Measurement	Remarks	Error
Pressure	Transducer and charge amplifier errors assumed small since directly calibrated. Oscilloscope calibration and trace reading.	- ∿±1.0%
Temperature	Error in pyrometer reading including that due to 50 Hz ripple and feed mechanism Trace reading 1%	∿±1.5% ∿±0.2%
Position	Lead pin measurement Timing	∿±0.3% ∿±1.0%
Synchronisation		∿±0.5%

Overall error (as a sum of above) : 4.5%

In addition to this table, uncertainties arise for $\lambda > 500$ (see Section 4.3.1) and when a shock is present (see Section 4.3.2).

Because, smaller deflections away from the peak conditions are measured, and furthermore synchronisation is more difficult in these regions, the sum of the overall errors is expected to be in the range of ±7% to 10%. One source of uncertainty, that of the effects of impurities on the experiments, remains difficult to assess as discussed in Ref.6. More will be said about impurities in Section 4.5.

3. COMPUTER PROGRAM AIDS TO THE EXPERIMENTS.

3.1 Piston compression cycle predictions

Calculations concerning the compression of the gas have been carried out using a piston cycle program. The basic program uses a 4th order Runge-Kutta numerical method to solve the system of two ordinary differential equations resulting from Newton's law describing the forces on the piston, including friction during the cycle. The program has been modified in several ways as described in Ref. 6 providing aids to the estimation of various sources of uncertainty and to the carrying out of the experiments.

3.2 Data reduction programs

Two main data reduction programs have been designed. One program uses inputs of the measurements of the traces as read directly from the measuring table and all the carefully determined calibration constants to calculate the raw data. The second program presents the results to allow comparison with appropriate equations of state.

1. Data reduction of raw data

The values of the state parameters are generated by introducing into the program the co-ordinates of the pressure, emission, absorption and position traces. The first three are introduced at equal time intervals; the latter is introduced as the time, arbitrarily referenced, for the distance transducer to sense the equal interval distances defined by the centre of the teeth and the grooves of the piston.

The following information, the acquisition of which is described in Ref.6, is also provided :

- oscilloscope and transducer calibration curves and values,
- lamp voltage and current, and lamp calibration curve,
- transmission coefficients of the optical system,
- crushed lead pin length,
- corrections for barrel expansion and piston compression due to the high pressures developed.

The reduced data is then re-arranged in equal interval time steps by using a four-point interpolation procedure. The data can be plotted out on the VKI line printer to the resolution available on the printer itself. The main use of this plot was to give a quick look of the data (without laborious plotting) and to indicate where errors in transcribing the raw data from the traces may have occurred. A sophisticated curve plotter for presenting the results with better resolution was not readily available at VKI.

The units selected to present the reduced gas state data were kg/cm^2 for pressure, amagats (defined as density of the gas, i.e. N_2 or air, at standard conditions[x]) for density and K for temperature.

---

[x] Standard conditions :

p_o = 1atm = 1.03323 kg/cm^2 = 760 mm Hg = 101324.6 N/m^2

T_o = 273.15 K

Then 1 amagat = 44.5868×10^{-6} gm - mole/cm^3

i.e. 1 amagat for N_2 = 1.24903×10^{-3} gm/cm^3

and 1 amagat for air = 1.29143×10^{-3} gm/cm^3

It has been discussed in Ref. 6 that despite the electronic synchronisation of traces carried out, the peak temperature did not coincide exactly with the peak pressure and density. Since it is difficult to synchronise the data to better than of order 10 μsec it was suggested that the data should be re-aligned such that the peaks did coincide. The philosophy for this is that provided the test slug is homogeneous, it is difficult to conceive that the temperature will be rising whilst the pressure and density are falling. For this reason, a modification was made to the program to re-align the data. This was carried out by finding an average axis of symmetry around the peak. Values of time have thus been re-calculated with respect to this common axis for presentation both in the computer plots and in the second part of the data reduction outlined below.

2. Comparison between experimental data and theoretical equation of state

A computer program was devised to aid the comparison of theoretically determined equations of state with the experimental results. It calculates for each measured point (P, ρ, T) the following parameters : $P_{calc}(\rho_{meas}, T_{meas})$ i.e. calculated pressure from measured density and measured temperature; $\rho_{calc}(P_{meas}, T_{meas})$; and $T_{calc}(P_{meas}, \rho_{meas})$. Also the entropies $S_1/R\ (\rho_{meas}, T_{meas})$, $S_2/R(P_{meas}, T_{meas})$, $S_3/R(P_{meas}, \rho_{meas})$ are calculated.

The theoretical thermodynamic information used for nitrogen was the Enkenhus-Culotta equation of state (Ref. 4) which agrees with the AEDC tables (Ref. 7) to within a few

per cent for all parameters over the range considered. Two subroutines give pressure and dimensionless entropy as a function of density and temperature. For air, the AEDC tables (Ref. 8) were used. A four point interpolation formula gives pressure and dimensionless entropy as a function of density and temperature. In each case a Newton-Raphson searching procedure is used to calculate ρ_1, T_1, S_2/R and S_3/R when the arguments are not density and temperature.

An example of the read out of the complete data reduction program is given in Table 1 placed at the end of the report.

4. RESULTS AND DISCUSSION

4.1 Isentropicity of compression cycle

Further observations of oscillations around the mean pressure variations, similar to those reported of Ref. 6 have been sensed for low entropy cases as illustrated in Fig. 4. These cases are characterised by their high initial test gas pressure requiring greater piston velocities to achieve the desired conditions. Further calculations using the cycle prediction program in which the full characteristics method was applied to the flow of gas in front of the piston (which for simplicity was assumed perfect) showed that weak shock waves can be developed in the later stages of the compression for these high piston speed cases (i.e. greater than 30 m/sec).

Further examination of the traces indicates that although abrupt pressure steps, indicative of shock waves, are not seen the waves, being only weak ones, are indeed sensed by the transducers but smoothed by the limited response (for such sharp rise times) of the pressure measuring system . Further similarity in experiment and theory was found, in that these weak shocks damp out quite rapidly during the early stages of the expansion process. These shocks could be reduced in strength by increasing the piston weight, however this was not attempted because of the limited length of piston that could be introduced into the facility, as well as causing a problem of decreasing the test gas sample. Temperature and piston position measurements do not so obviously show up these oscillations. In the former casethis is because the oscillation frequency tends to be of

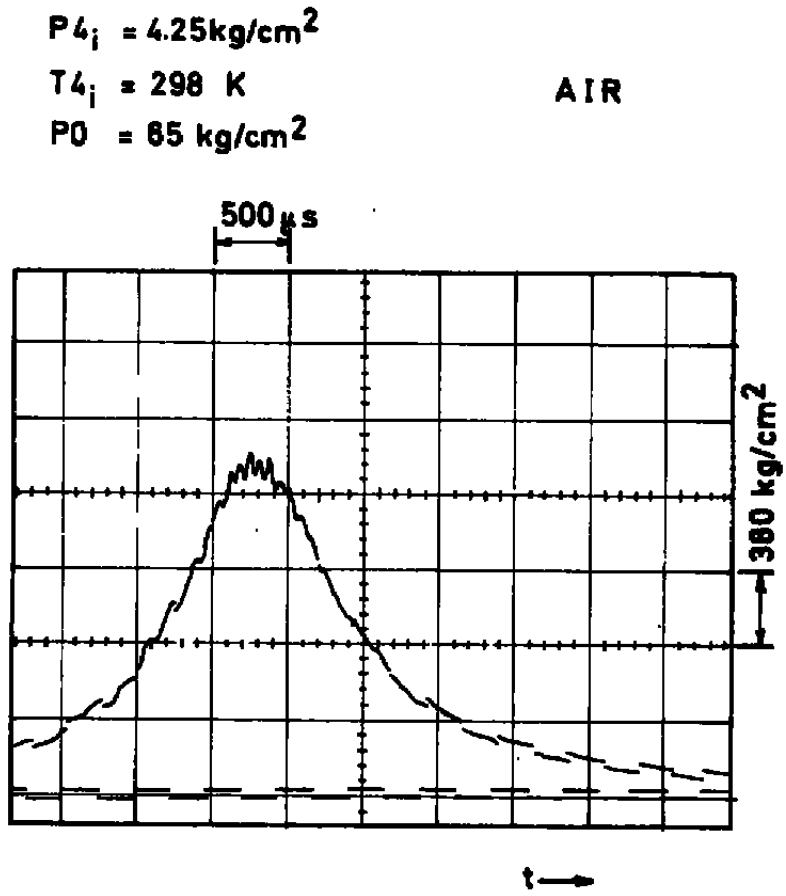

FIG. 4. Pressure trace when piston speed is high.

the same order as the chopping system. In the latter case the motion of the piston is an integral function of the pressure trace and hence will be highly smoothed.

The complete calculations have not as yet been carried out because of the difficulty in introducing the Rankine-Hugoniot relations to account for flow through shock waves which are curved (since they are moving through an accelerating gas) and reflected from the moving boundary of the piston. The solution is possible, but considerable development and computing time is required.

The main consequences of this formation of shocks are :

- the cycle will no longer be isentropic; small increases in entropy will occur;
- the sample will be non-homogeneous, causing larger uncertainties than expected;
- transport properties , assessed from slopes of data from expectedly isentropic compressions and expansions, will become inaccurate;
- analysis of the basic data using the expectedly good assumption that the cycle is isentropic should be treated with caution.

The degree to which the formation of shocks upsets the sometimes required assumption of homogeneity and isentropicity has not as yet been assessed. However further comments are given in Section 4.5.

4.2 Some observations concerning the temperature measurement

A typical temperature measurement trace at conditions of high temperature and pressure is illustrated in Fig.5. It is seen that at the period during and near the peak temperature then v_1 is equal to v_3. As pointed out in Ref.5 this indicates that, during this period, maximum absorption of the light from the lamp occurs. The equation for the gas temperature :

$$\frac{1}{T_s} = \frac{1}{T_L} + \frac{k}{h\nu} \ln \left(1 + \frac{v_2 - v_3}{v_1}\right) \qquad \text{(from Eq.1 in Ref.6)}$$

becomes

$$\frac{1}{T_s} = \frac{1}{T_L} + \frac{k}{h\nu} \ln \left(\frac{v_2}{v_1}\right)$$

This equation may be shown to be valid, but the measured temperature is then not an average temperature over the optical path length in the compression chamber but an average temperature over the "optical depth" of the emitting sodium atoms. Provided that no significant gradients exist in this "depth", the measured temperature is still indicative of the test gas temperature and no additional error is incurred in this case. This condition, v_1 equal to v_3, occurs at combined high temperature and pressure conditions as illustrated in Fig.6. The condition has an advantage of making the temperature measurement independent of the lamp-light chopping speed. Advantage has been made of this "black-body" method to measure temperatures in helium for temperatures greater than 2500 K (Ref.12).

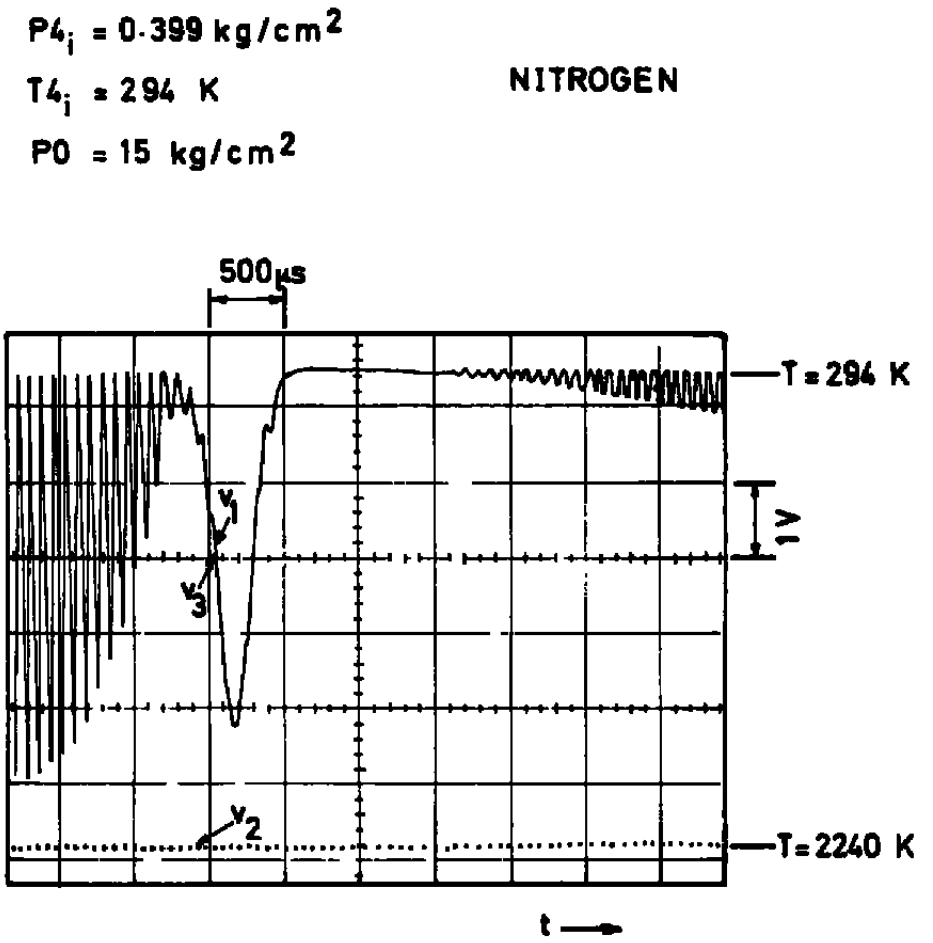

FIG.5 - Typical high temperature trace.

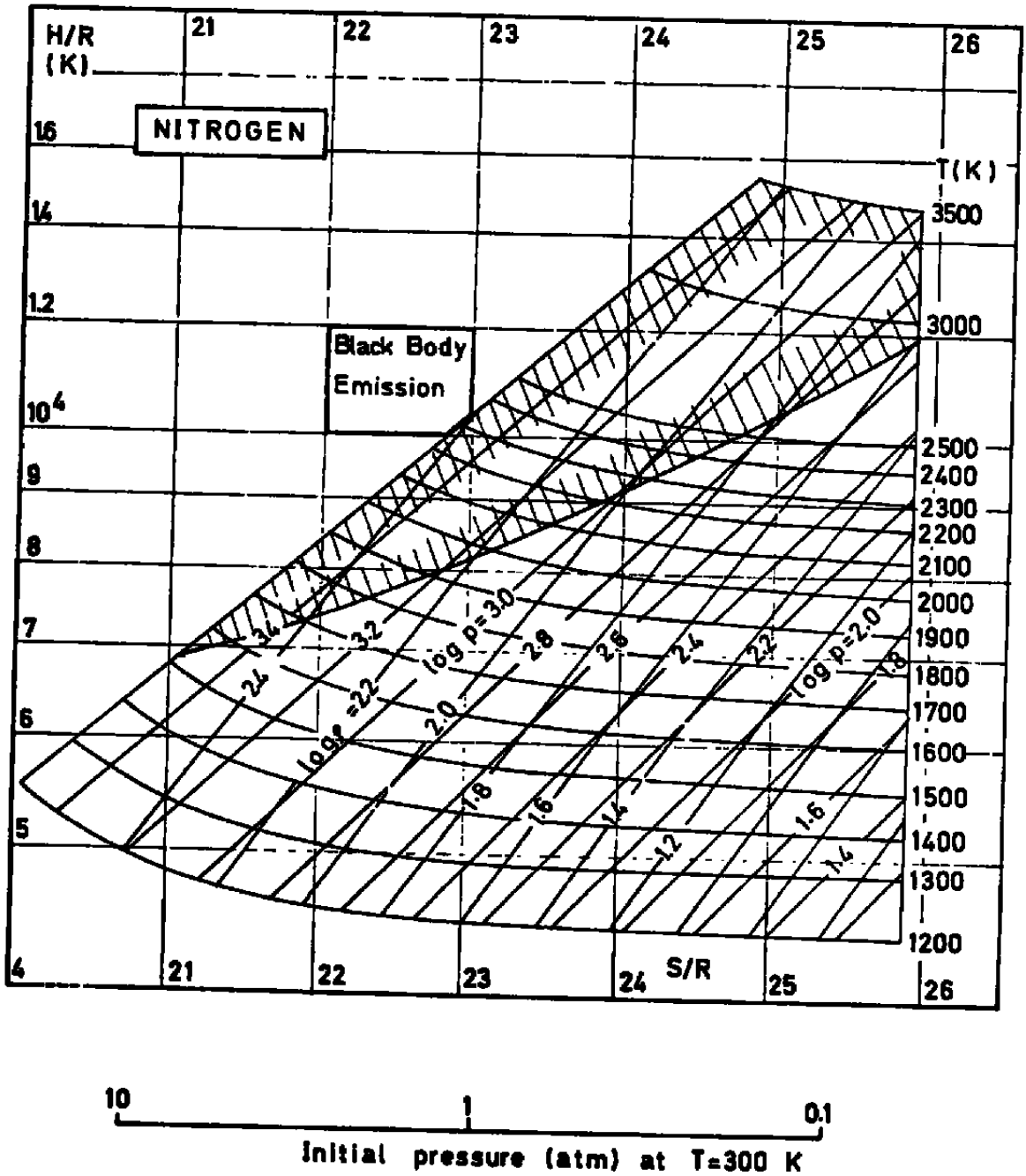

FIG. 6: Regions on Mollier Chart at which "Black Body" measurement occurs - a) Nitrogen

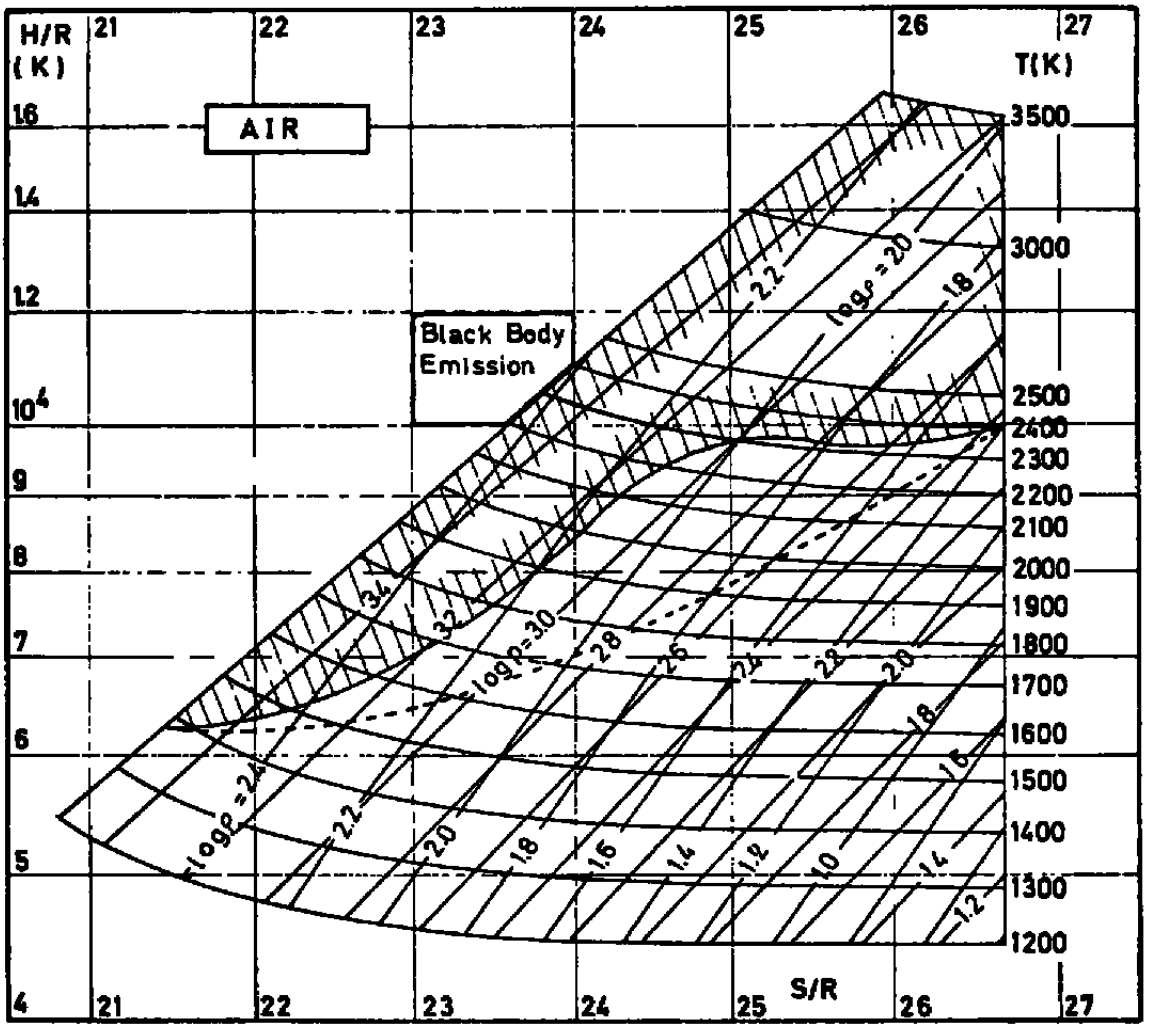

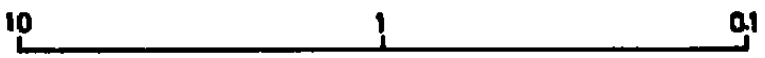

Initial pressure(atm) at 300 K

FIG.6: Regions on Mollier Chart at which "Black Body" measurement occurs - b) Air

Black Body emission is thougth to extend to the dashed line if no chemical reactions or impurities were present.

If maximum absorption does not occur (i.e. $v_1 \neq v_3$ near the peak) then the traces have a shape, similar to that shown in Fig. 7. In all the nitrogen traces, good symmetry of the emission trace is obtained, however this is not found in air cases. In all cases (nitrogen and air) away from the peak conditions, asymmetry of the absorption trace, however, is obtained; more absorption occurring after the peak than before. This asymmetry has been discussed in detail in Ref. 6, in which high level turbulence, impurities arising from ablation etc. during the expansion part of the cycle have been blamed for the anomaly. For this reason more reliance is placed by the authors on the data during the compression part of the cycle.

4.3. Further discussion on measurement uncertainties

4.3.1 Uncertainties arising from small volumes of gas samples

At high entropy level cases, at high temperature conditions the minimum volume of the compressed sample becomes so small that the piston approaches the end of the tube. The resolution of the sensors measuring piston motion then approaches the value to be measured, hence inaccuracies arise. Inaccuracies become important when the piston approaches to less than 3 mm from the end wall equivalent to a compression ratio [x] of approximately 500 for N_2 and air.

---

[x] The compression ratio can be calculated from the data reduction program as the density measured during a test to the initial density.

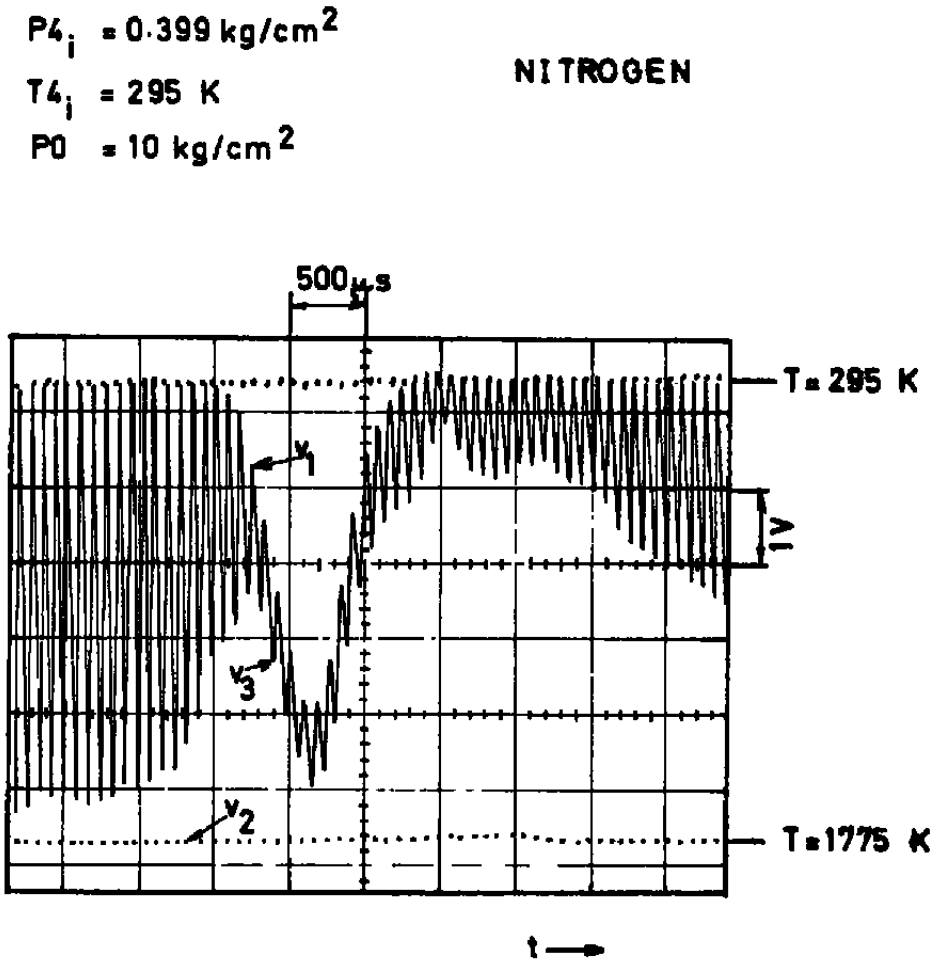

FIG. 7 - Typical non black body temperature trace.

The enclosure for the temperature measurements has a relatively small volume i.e. equivalent to a length of tube of approximately 0.04 cm. The limit of $\lambda = 500$ is shown on the H-S diagram illustrated in Fig.8. This limit aligns approximately with the $T_4 = 2700$ K line. This finding tends to nullify the usefulness of the carbon arc light source for extending the range of temperature to 3500 K using this particular facility.

4.3.2 Uncertainties due to the presence of shock waves

As discussed in Section 4.1 there is evidence that shock waves are formed at the cases in which the piston speed is the highest, i.e. low entropy, high initial pressure conditions. In the data reduction the philosophy was taken to take the mean reading through the oscillations occurring especially in the pressure traces. In most cases the oscillations are no larger than the trace width and hence for these cases the error will not be large. The largest fluctuations seen are ±5% at the conditions S/R = 22.5, pressure 1660 kg/cm^2, temperature 1660 K and 219 amagats (as shown in Fig.4). The regions in which piston speeds are greater than 30m/sec corresponding to shock formation are presented in Fig.9. In nitrogen, the limit aligns approximately with the S/R = 22.5 line and in air with the S/R = 23.5 line. However, the overall error does not exceed 5% if these limits are decreased to the S/R = 22 and 23 lines respectively since the shock is very weak (less than 0.5%) for entropy values larger than 22 and 23 respectively.

4.4 Presentation of Results

Table 2[x] summarises the tests in which measurements of the state of the dense high temperature gases were made. The initial

[x] presented at the end of the report.

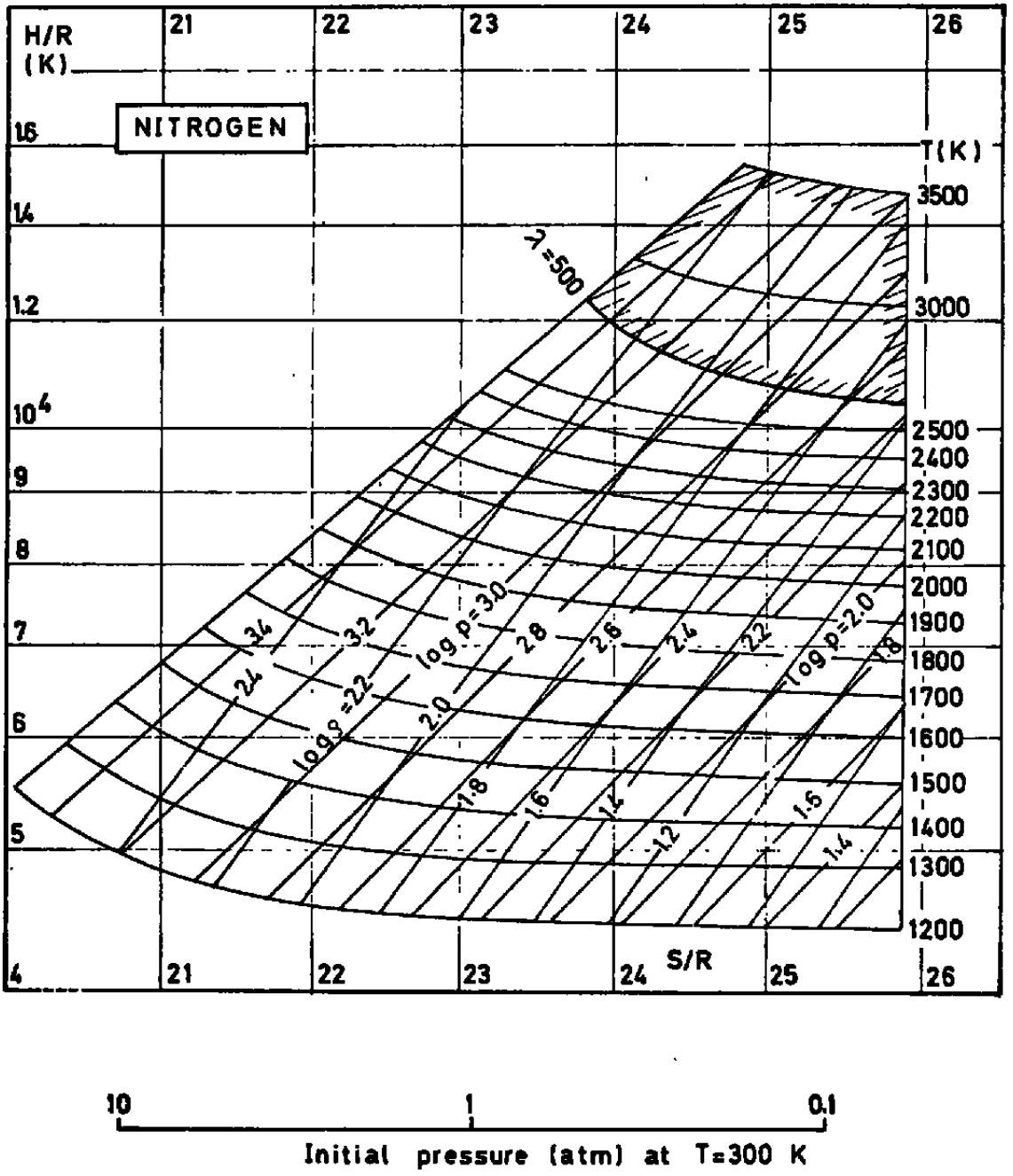

FIG.8: Conditions on Mollier Chart at which $\lambda > 500$

a) Nitrogen

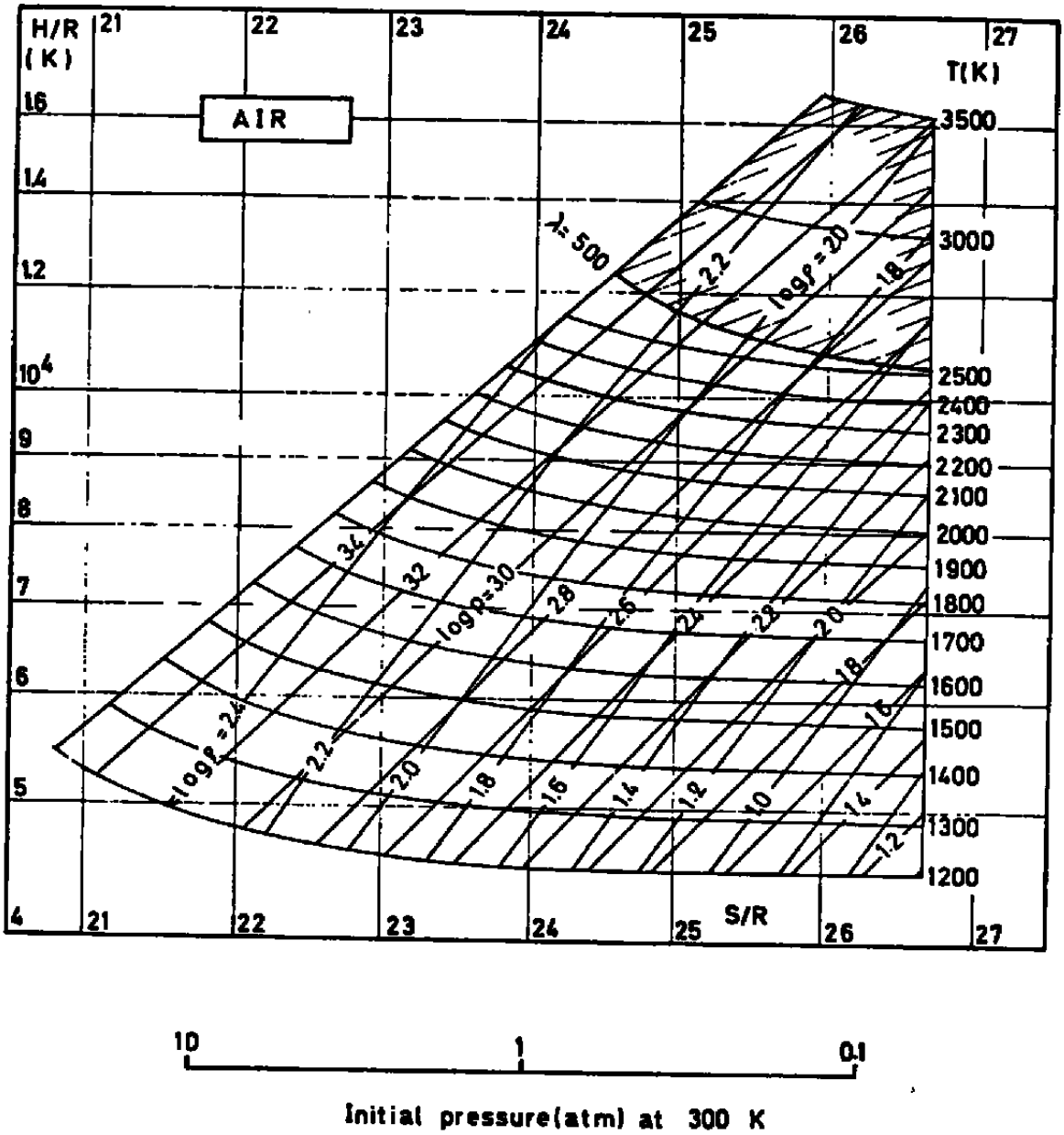

FIG.8: Conditions on Mollier Chart at which $\lambda > 500$

b) Air

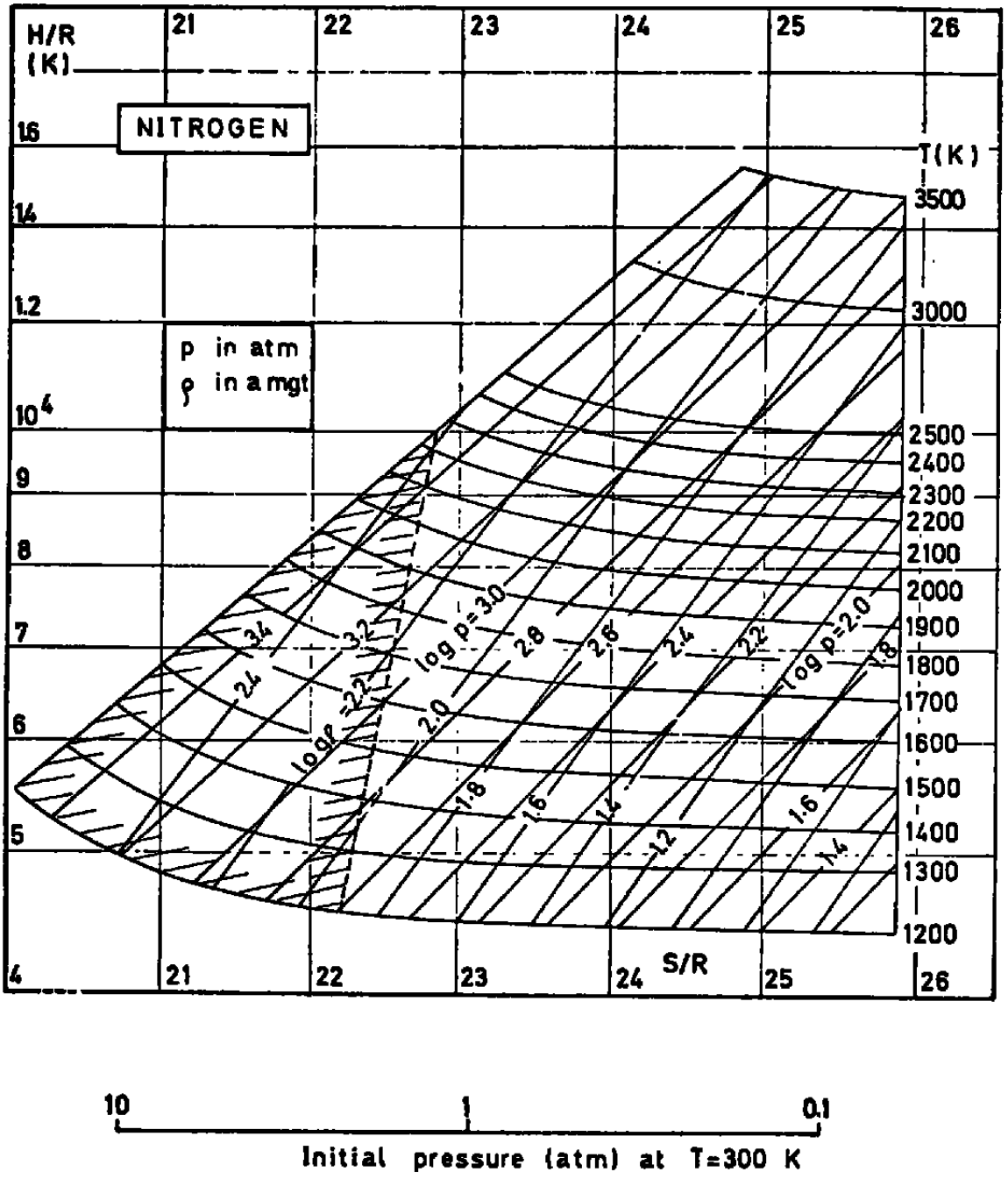

FIG.9a - Region where a weak shock forms during the compression stroke in nitrogen

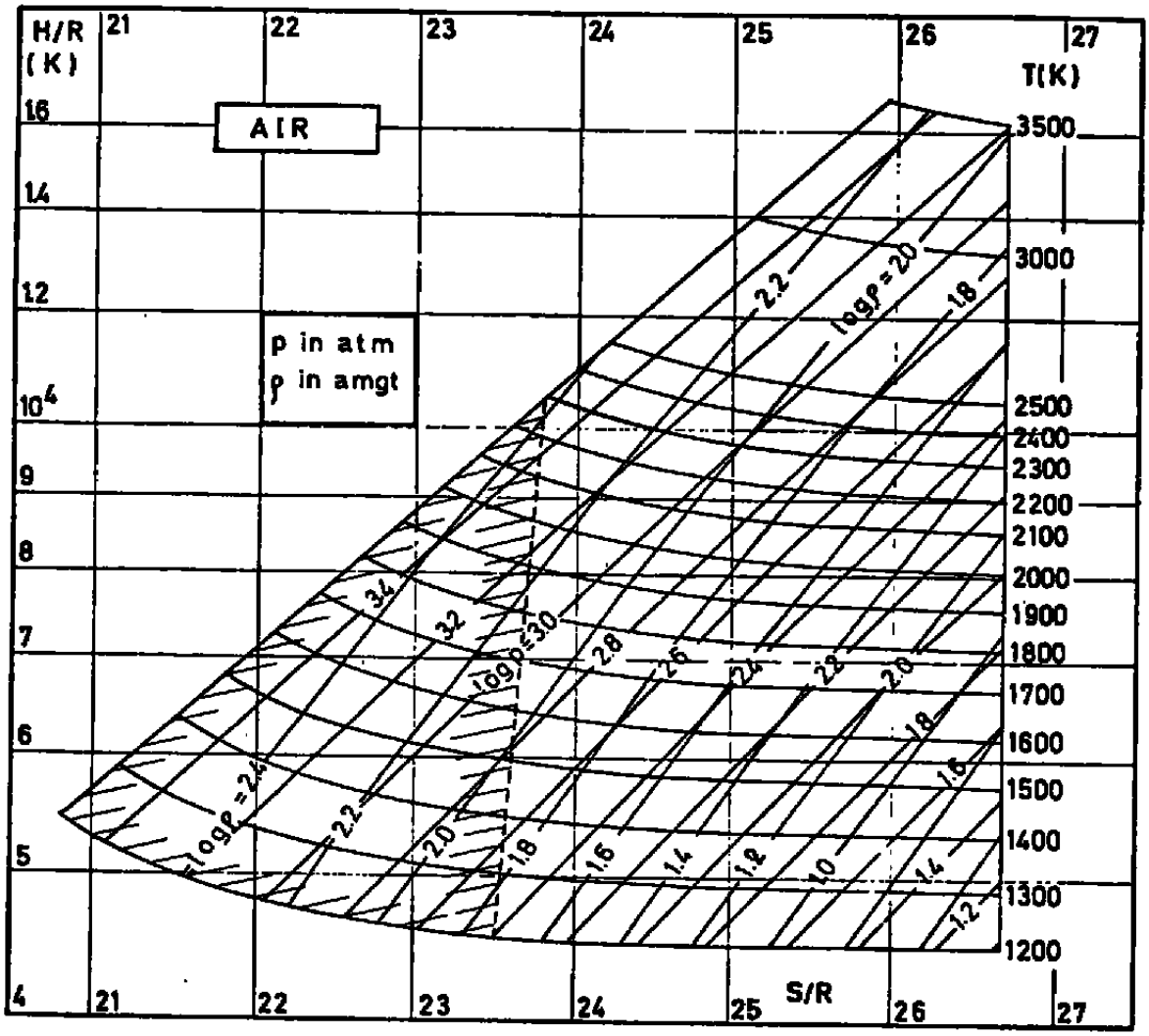

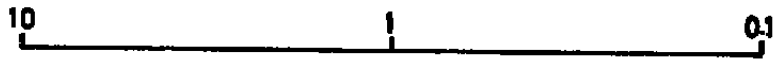

Initial pressure(atm) at 300 K

FIG-9b-Region where a weak shock forms during the compression stroke in air.

conditions and the maximum measured values of pressure , density and temperature are there presented. The range of the tests carried out in this series is illustrated in an H-S diagram (Fig.10) by plotting the range of pressures achieved during every test at the initial dimensionless entropy of the sample. Because away from peak conditions, errors are greater than 4.5%, vertical thick bars have been used instead of lines. The data reduction of all these tests using the method described in Section 3.2 and plots of results has been carried out, and copies of the very extensive complete set of results rest at VKI and AEDC.

The plots of peak measured values of pressure, density and temperature against their values calculated from the other two measured parameters (equivalent to Figs. 21, 22, 29, 30 of Ref.6) revealed only that even larger differences, but with similar trends, are seen over this extended range of conditions. It was considered that no usefulness would be gained by plotting this extensive data in this report, in view of more useful plots presented in the next section.

4.5 Discussion

The aim of this study is to provide new experimental data to compare with proposed models of the equations of state at conditions well outside those investigated in detail previously. The accuracy of these theoretical equations of state remains unverified. In order to determine the state of a gas, at least three parameters must be known. In these experiments pressure and temperature were measured directly and density inferred from measurements of volume of a known constant mass of gas. Great attention was paid to keeping the uncertainties as small as possible, and to ensuring the quality of the sample. When all of the information has been obtained severe problems

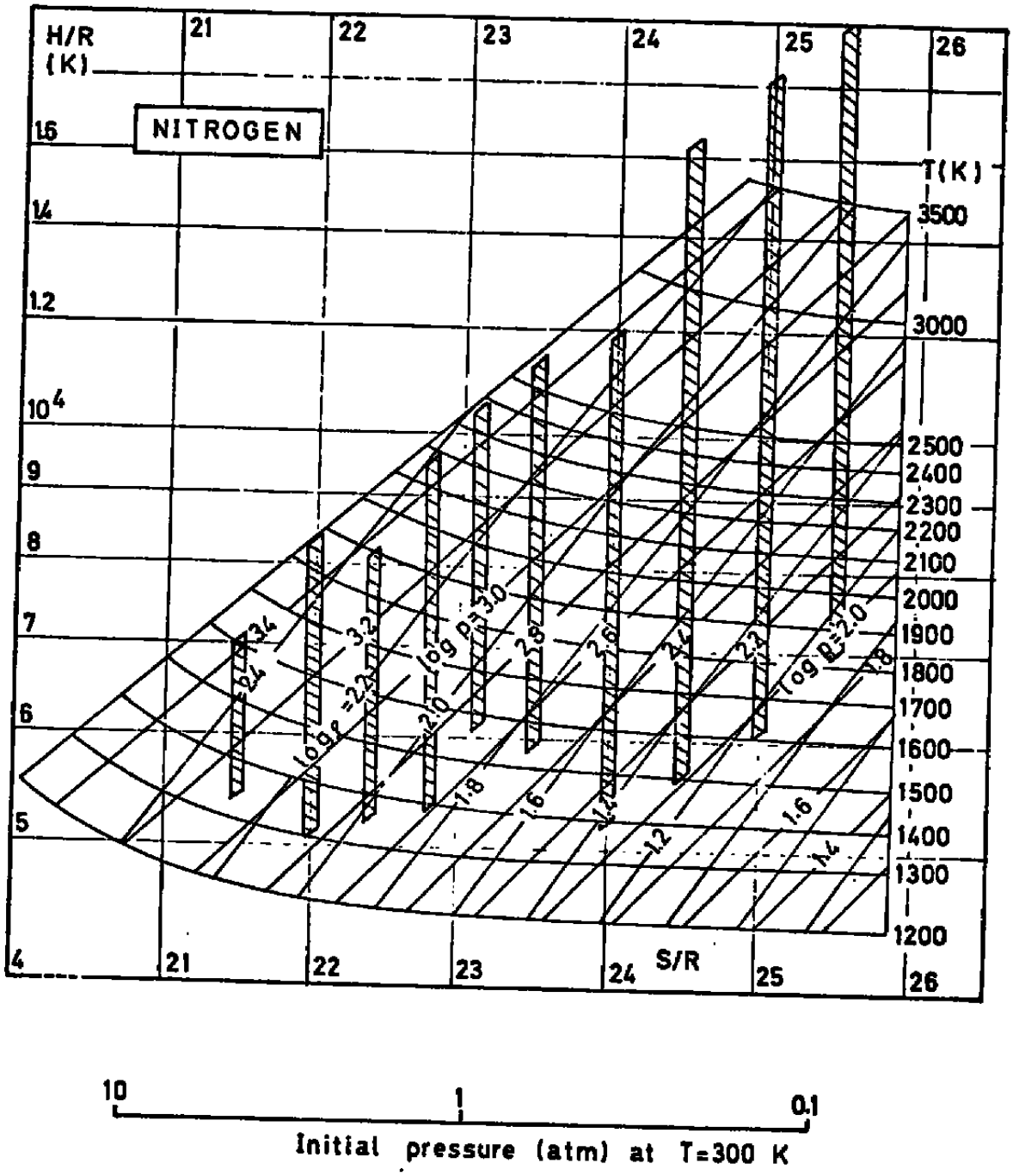

FIG 10: Summary of conditions tested - a) Nitrogen

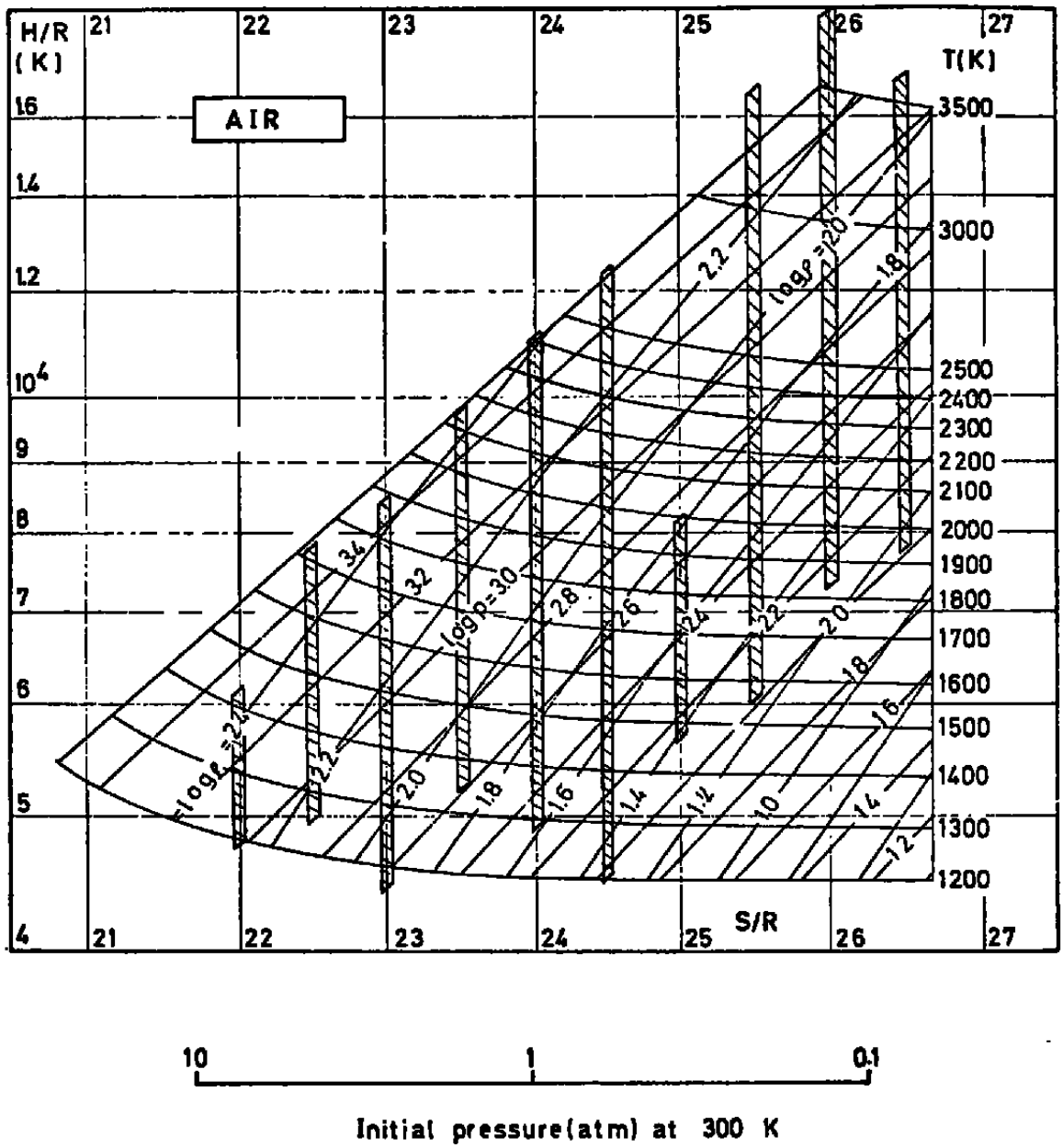

FIG.10: Summary of conditions tested - b) Air

exist in selecting a method of comparing the three parameter experimental results with the models. One of the chief difficulties is to ascertain where the errors lie if there are discrepancies arising; they may be in the development of the sample, the measurements of properties of the sample or in the actual model itself. Another difficulty that may arise is that even if there is agreement to within the assessed uncertainty of the experiment, there may be the chance that an error in one parameter may be offset by another. However in the latter case, such a state of affairs will be unlikely if agreement is found in many tests taken over a broad range of conditions.

The approach taken in the early stages of this research (Ref. 6) was to compare the measurement of one parameter (either P, ρ or T), with the calculation of it from the other two measured parameters using the model for which verification is desired. The problem with this is that if differences do occur then it is difficult to decide whether it is due to an error in the model, or one error or an accumulation of errors in the experiment. In fact as was pointed out in Ref. 6 systematic deviations from the models are indeed obtained at conditions typically above 1700 K and 1400 kg/cm^2 for S/R between 22 and 23.5. The results over an extended range (S/R from 21.5 to 25.5) show even larger deviations as noted in Section 4.4. Air tests show larger and less systematic deviations than for the nitrogen tests.

A parameter known fairly accurately, but as yet unused in the comparison with the real gas equation of state is the entropy. The compression is essentially isentropic, such

that the initial value of entropy, which can be defined very accurately from the initial running conditions, will remain constant throughout the compression and expansion. Small rises in entropy are expected in the low entropy cases during a test due to the formation of weak shocks (see Section 4.1) and energy losses caused by heat transfer. In order to use this information then the data has been plotted in different forms. Figs. 11 and 12 illustrate for all entropy level cases for nitrogen and air respectively measured peak temperature plotted against peak pressure and compared against that predicted by the representative model equation of state. In Figs. 13 and 14 all entropy level cases are plotted for peak pressure and peak density. In Fig. 15, peak temperature is plotted versus peak density for two entropy cases. It is seen that for all cases in which the temperature measurement is included (illustrated by Figs. 11, 12 and 15), then deviations away from the equation of state models are produced. It should be noted that such deviations were seen for all entropy levels. However, it is seen that for all cases in which the temperature measurement is avoided (given in full in Figs. 13 and 14) very good agreement with the models are produced, except for high entropy, high compression ratio cases when large uncertainties are expected (see Section 4.3.2). It is pointed out that this latter plot is less sensitive to changes in entropy than in the previous two presentations given. However close scrutiny leads to the conclusion that better correlation is indeed obtained in this plot.

One interpretation of these observations is that the temperature measurement is in error. Possible connected conclusions arising from this interpretation and from the

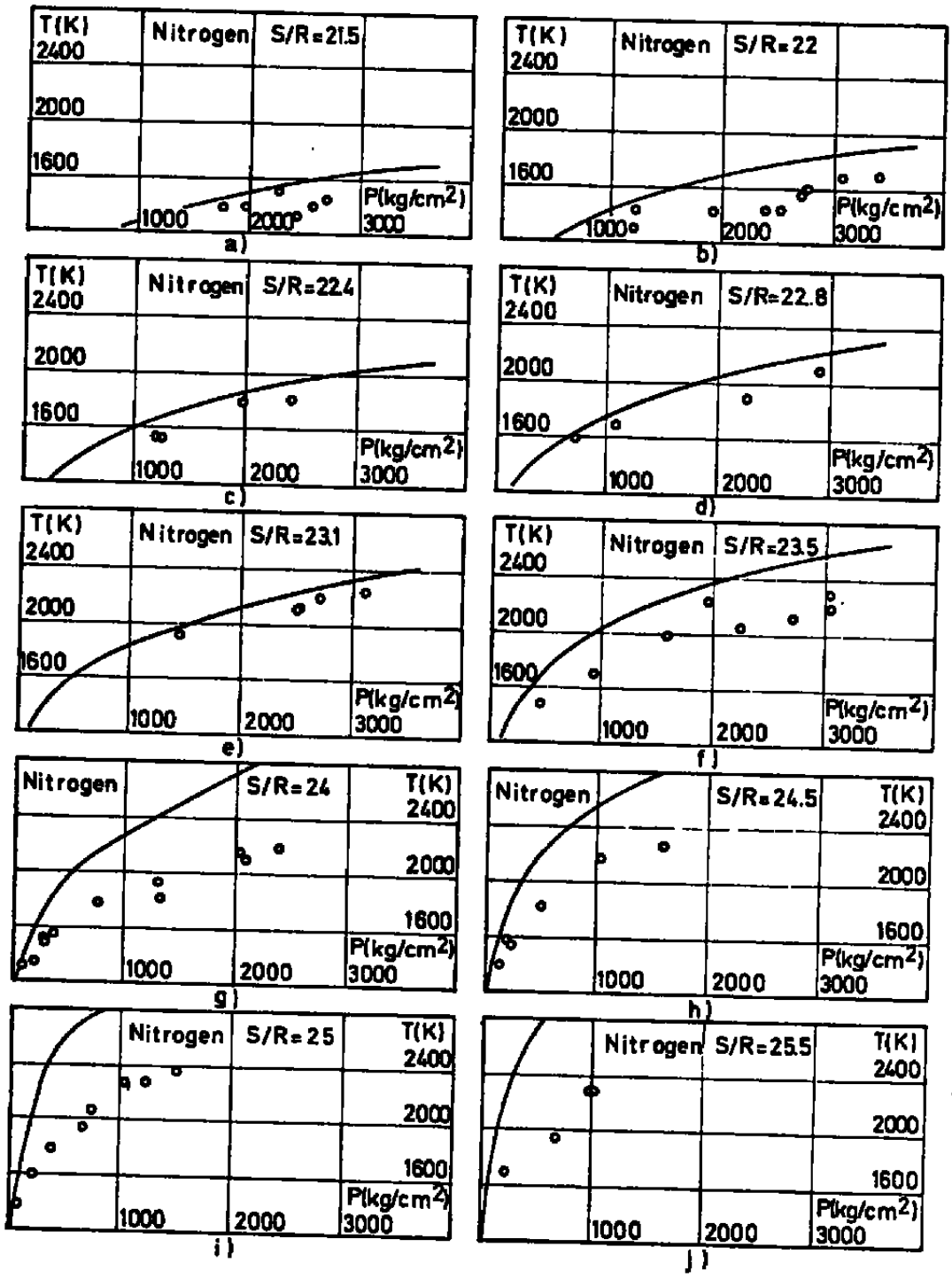

FIG.11 - Plot of peak temperature versus peak pressure in nitrogen.

• Experiment, — Equation of state (Ref. 7) at given S/R.

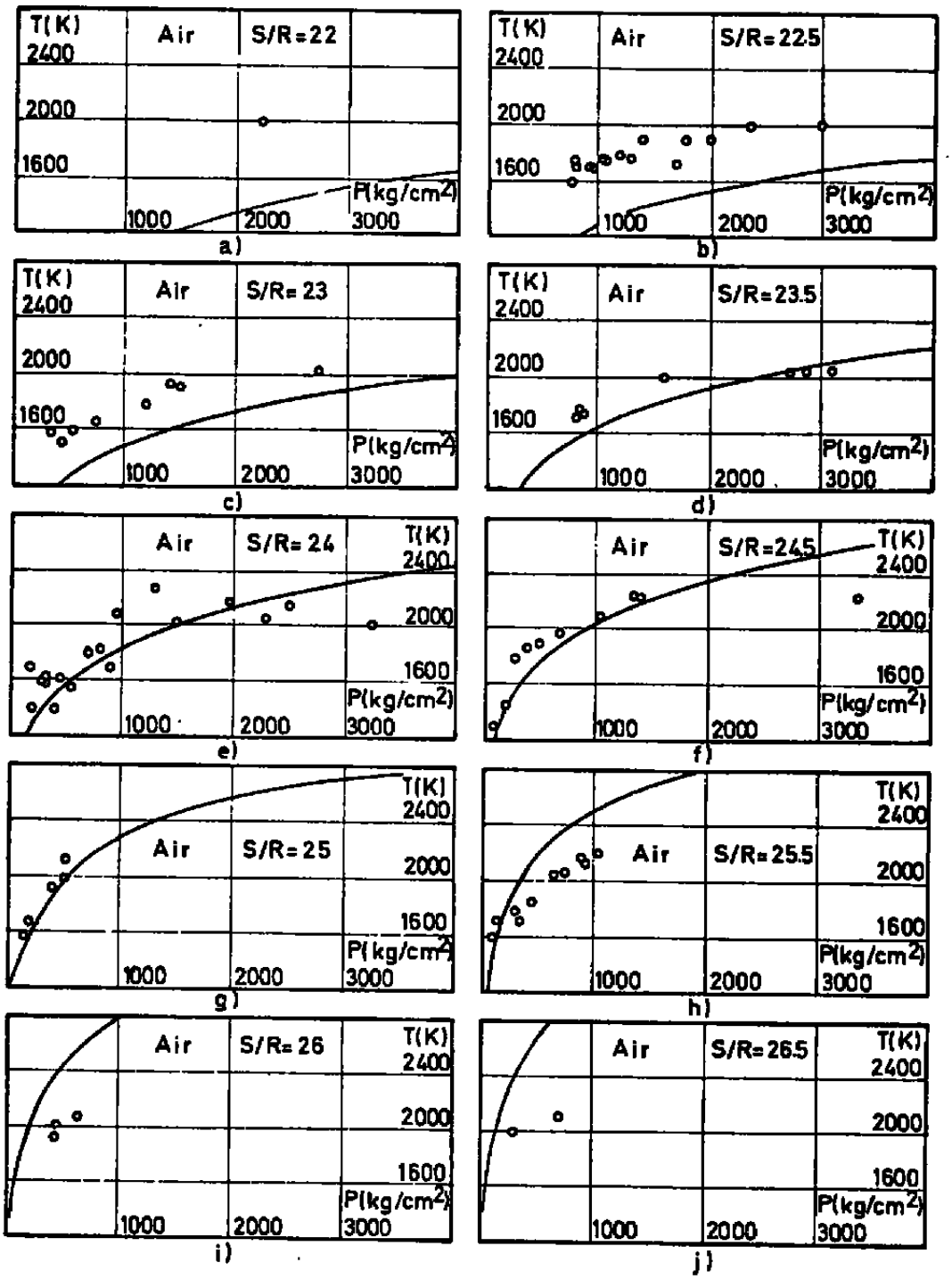

FIG. 12 - Plot of peak temperature versus peak pressure in air.

∘ Experiment, — Equation of state (Ref. 8) at given S/R.

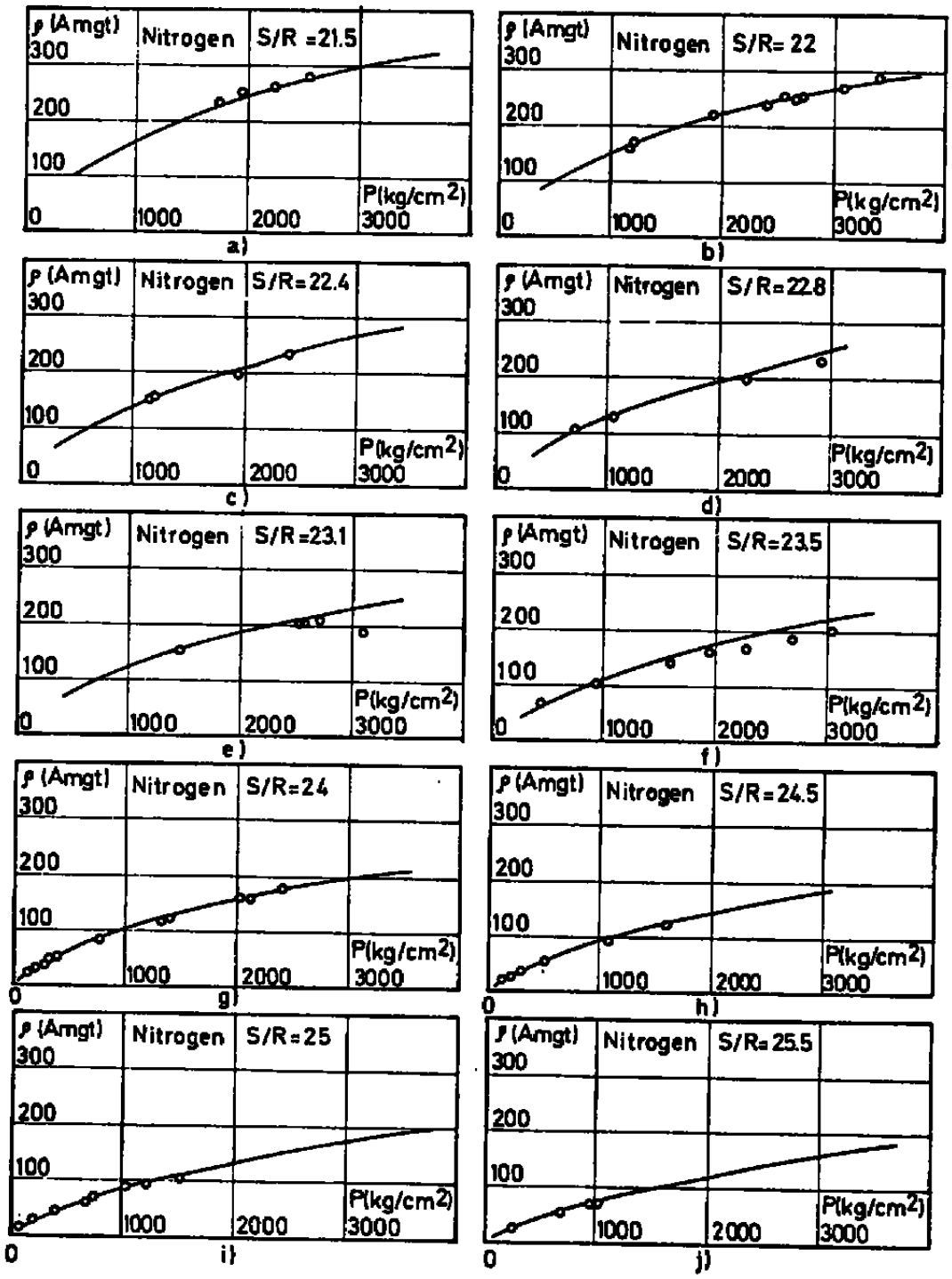

FIG. 13 - Plot of peak density versus peak pressure in nitrogen.

∘ Experiment, — Equation of state (Ref. 7) at given S/R.

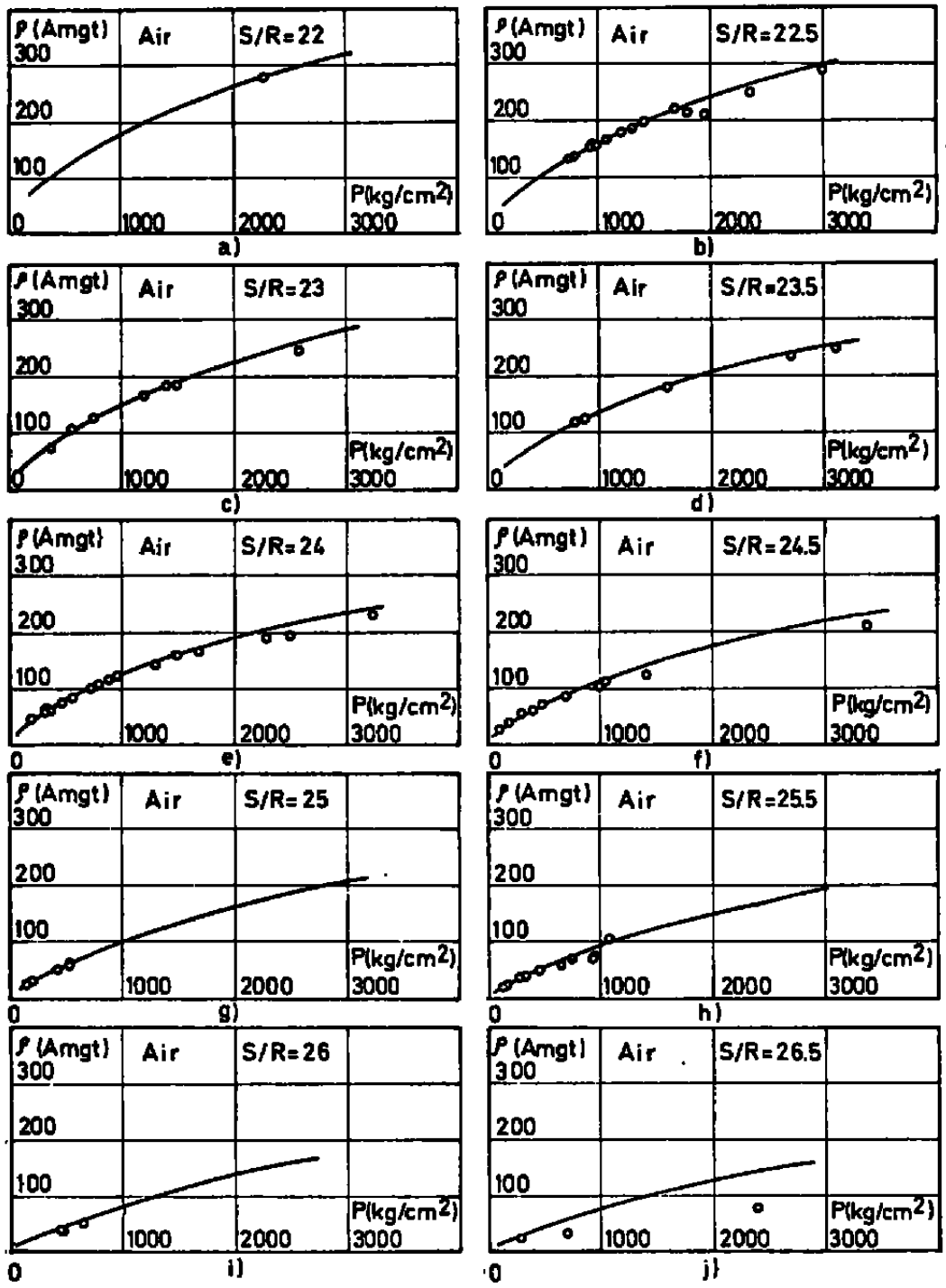

FIG.14- Plot of peak density versus peak pressure in air.

∘ Experiment, —— Equation of state (Ref.8) at given S/R.

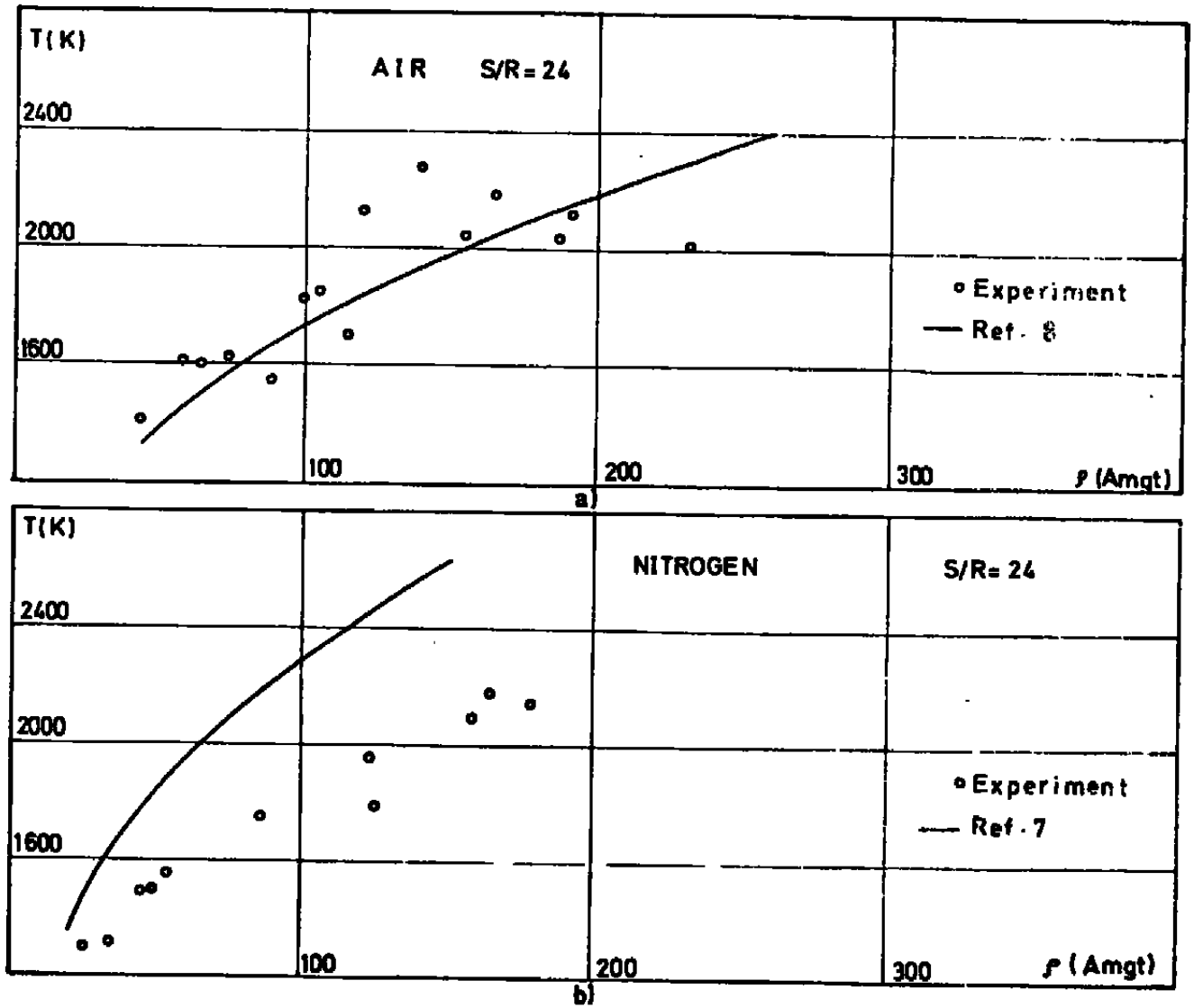

FIG. 15 - Plot of peak temperature versus peak density.

good agreement between experiments and the equation of state models are that :

a) the density and pressure measurements are accurate.

b) The compression tube produces a sample of dense high temperature gas which is sufficiently pure and homogeneous as to match the accuracy of the instrumentation measuring it.

c) The equation of state models selected are accurate.

The question now remains as to where lies the error in temperature measurement in this hypothesis. The lamp and optics are very carefully calibrated and in theory there appears to be little uncertainty in the concept of using sodium as the radiating substance in these high density gas samples. Various tare tests were carried out to verify that no errors were introduced by facility vibrations. However, no direct dynamic calibration of the method under operating conditions is available at present. The only possible means of calibration would be to apply another temperature technique at the same time as the sodium line reversal technique. A possible reason for errors in temperature is that impurities (not occurring in large enough concentrations to affect the overall thermodynamic characteristics of the gas sample) may be affecting the sodium emission and absorption of the light from the lamp. Little is known about the effect of impurities on the SLR method under conditions of high density. To the authors' knowledge this is the first attempt made and the effect may be rather sensitive to accuracy.

For all nitrogen tests, and the lower entropy

level air tests, the temperature is lower than expected (if pressure and density are measured accurately). Equation 2 illustrates that to give this result, either the light emission is too low or the light absorption is too high. The decrease in v_3 (which is a function of absorption) to give a 1 % increase in temperature is found to be 50 % at 2200 K. Similarly the decrease in v_1 (which is a function of the light emission) to give a 2 % decrease in temperature is found to be 50 % at 2200 K.

Several characteristics (noted before) may provide some doubt about the method of measuring temperature. One is that the absorption traces (and sometimes the emission traces) are unsymmetrical with respect to peak conditions in which more absorption occurs during the expansion than during the compression at equivalent pressure and density conditions (Section 4.2). However, in view of the insensitivity of the temperature to absorption pointed out in the last paragraph, this is thought not to provoke large errors. The other concerns the observation of emission in the sodium D-line bandwidth even when no sodium azide was placed in the tube and the test section cleaned thoroughly (See Ref. 6). Sophisticated time resolved spectroscopic photographic techniques, beyond the capability of VKI, are required to understand this problem. Even after such a study (likely to be very extensive) it may not, even then, be feasible to develop the sodium line reversal technique to sufficient accuracy, hence it is thought more cost-effective to examine other possibilities for measuring temperature.

Another interpretation of the poor comparison of experiments with the equation of state model when the

temperature measurement is included, but good comparison when the temperature is suppressed may be again associated with impurities. In this case the impurities may be so large that the quality of the gas sample is impaired but the pressure, temperature and density measurements are accurate. Less weight is given to this interpretation for at least the nitrogen tests by the uniformity of the correlations of Fig. 13. This interpretation has more weight for the air tests since some inconsistency of results is seen.

5. CONCLUSIONS

The compression tube has been shown to be capable of generating samples of air and nitrogen test gases up to 3000 kg/cm^2 and 3500 K. Results of measurements of pressure using a piezo-electric sensor, temperature using a sodium line reversal technique and density using an eddy current distance transducer, show discrepancies on comparison with advanced equation of state models. By using knowledge of the entropy of the sample it was illustrated from data correlations that the discrepancies most probably arise from errors in temperature measurement. Such errors are surmised to occur through the sensitivity of the spectroscopic technique to slight impurities at high density conditions. Tentative conclusions arising from these successful correlations are that the transient method of generating dense high temperature samples is suitable and the pressure and density measurements and the gas models are accurate. Further experiments using a non-spectroscopic technique for measuring temperature are necessary, however, to confirm this satisfactory conclusion and reject other possible but less satisfactory interpretations of the data.

An attempt was made to increase the temperature measuring capability to 3500 K, but in view of the preceding remarks, and the fact that large inaccuracies in the density measurement are expected at such high temperatures in this facility, the usefulness of this phase of the study was nullified.

REFERENCES

1. LUKASIEWICZ : "Experimental Methods of Hypersonics" M. Dekker, New York 1973.

2. DAVIDSON : "Statistical Mechanics" Mc Graw Hill, 1962 Chapter 16-20.

3. BEATTIE, J.A. : "Thermodynamic of Real Gases and Mixtures of Real Gases". Thermodynamics and Physics of Matter, Princeton Series on High Speed Aerodynamics and Jet Propulsion. Vol.1, F.D. Rossini Editor, 1955.

4. CULOTTA, S.; ENKENHUS, K.R. : "Analytical Expressions for the Thermodynamic Properties of Dense Nitrogen". VKI TN50 Sept. 1968.

5. LEWIS, M.J. ; ROMAN, B.P.; ROUEL, G.P. : "Techniques for Measuring the Thermodynamic Properties of a Dense Gas" VKI TM23 May 1971 or : International Congress on Instrumentation in Aerospace Simulation Facilities : ICIASF 71 Record.

6. ROUEL, G.P.; RICHARDS, B.E. : "Study of the real gas effects of nitrogen and air at high densities and temperatures". AEDC Scientific report N° 1, Grant AFOSR 72.2413. (to be published as AEDC TR)

7. GRABAU, M; BRAHINSKY, H.S. : "Thermodynamic Properties of Nitrogen from 300 to 6000 K and from 1 to 1000 Amagats". AEDC - TR - 66 - 69 August 1966.

8. GRABAU, M.; BRAHINSKY, H.S. : "Thermodynamic Properties of Air from 300 to 6000 K and from 1 to 1000 Amagats". AEDC - TR - 66 - 147 January 1967.

9. GAYDON, A.G.; HURLE, I.R. : "The Shock Tube in High Temperature Chemical Physics". Rheinhold Publishing Co., N.Y. 1963.

10. NULL, M.R.; LOZIER, W.W. : "The Carbon Arc as a Radiation Standard", Temperature, its Measurement and Control in Science and Industry, Vol 3, Part 1, p.p. 551-558 (Rheinhold Pub. Co.).

11. HANKINS, M.A. : "The pyrometric Molarc radiation standard at 3800 K". Mole-Richardson, California, Bulletin N° 2371.

12. ROMAN, B.P.; ROUEL, G.P.; LEWIS, M.J.; RICHARDS, B.E. : "Compression of Helium to High Pressures and Temperatures using a Ballistic Piston Apparatus". Sept. 1971 VKI Preprint 71-7.

TABLE 1 : TYPICAL READOUT OF DATA REDUCTION PROGRAM

TEST 12 RECORD 126 FILE ARRB5 GAS NITROGEN GUESSED INITIAL ENTROPY LEVEL S/R=23.1
P4I= 1.0000 KG/CM2 T4I=296 00 K R4I=0.090 ANGT EFFECTIVE S4I/R=23 090

TIME	PRES	TEMP	TIME	DENSITY
-252 3	713 4	1703.9	-664 2	40 43
-227 5	779 0	1721 4	-647 1	49.00
-202 0	847 2	1738 7	-624.2	51.24
-178.1	910 0	1756.4	-604.0	52.77
-153 3	1017 7	1785.4	-582.2	54 39
-128 6	1003 3	1802.4	-560 7	56.12
-103 9	1196 1	1824 0	-541 0	57.96
-79 1	1316 7	1846 0	-517 0	59 90
-54 4	1442.6	1874.4	-496 2	62.02
-29 7	1584 3	1901.1	-473 2	64.29
-4 9	1691 0	1927.6	-451 0	66.71
19 8	1778 4	1963 3	-426 2	69.33
44 5	1959.3	1997 3	-402.7	72.16
69 2	2116 7	2021.5	-379 9	75.23
94 0	2290 9	2043.6	-394.3	78 57
118 7	2365 9	2061.0	-328 2	82 23
143 4	2463 0	2075.7	-303 4	86.24
168 2	2510 2	2084 9	-277.6	90.65
192 9	2520 7	2090.7	-254 1	95 59
217 6	2504 9	2091.4	-227 6	101.00
242 4	2455 1	2087.7	-201 5	107.11
267 1	2242 2	2081.3	-175.7	114 00
291 8	2213 0	2070 0	-142 5	121.01
316 6	2074.0	2055 9	-111 9	130.70
341 3	1935.7	2032.0	-77.7	141 14
366 0	1791.5	1992 2	-41 6	153 26
390 7	1673 4	1956 5	0 0	167.65
415 5	1534 4	1924 5	51 9	184.09
440 2	1413 0	1889.0	203.7	206.06
464 9	1274 0	1870 3	334 7	184.91
489 7	1189.3	1843 3	366.5	167 58
514.4	1072 0	1811.9	441 1	153.34
539 1	991.5	1788 1	470 4	141.22
563 9	910 0	1761 6	512 3	130 03
588 6	855.1	1736 9	544 9	121 03
613 3	823.6	1709.0	577.1	114 02
638 1	729.2	1690.9	607 7	107.11
			636 1	101.02
			664.3	95 56
			692.2	90 57
			719.3	86 25
			745.4	82 24
			773.4	78.59
			798 3	75 25
			823.1	72.10
			847 6	69.29
			871 0	66.73
			894 0	64 31
			929 5	62.09
			953.4	59.95
			973.7	57.90
			990 2	56 14
			1010 0	54.41
			1041.7	52.74
			1062 2	51 26
			1082 0	49 01
			1109 1	48.49

TEST 12 RECORD 126 FILE ARRIL GAS NITROGEN GUESSED INITIAL ENTROPY LEVEL S/R=23.1
P4I= 1.0000 KG/CM2 T4I=296 00 K R4I=0.090 ANGT EFFECTIVE S4I/R=23 090

TIME	PRES	TEMP	DENS	P(R,T)	T(R,P)	R(T,P)	S(P,T)	S(R,T)	S(R,P)
-252 3	713 4	1703 9	95.92	706.5	1720 6	96 75	23 104	23 114	23.146
-227 5	779 0	1721 4	101 02	757.2	1770.9	103.56	23 059	23 080	23 100
-202 0	847 2	1738 7	106 79	815.1	1807 8	110 41	23 017	23 036	23 102
-178 1	910 0	1756.4	113 40	882 0	1826.3	117.26	22 980	23 015	23 146
-153 3	1017 7	1785 4	119 16	951.0	1910 4	126.21	22 946	23 014	23 236
-128 6	1003.3	1802.4	123.75	1022.9	1980 5	131.95	22 924	22 981	23 169
-103 9	1196 1	1824 0	133.16	1108.5	1968 0	141.78	22 877	22 953	23 261
-79 1	1316.7	1846 0	140 60	1195 0	2027 6	151 93	22 830	22 924	23 233
-54 4	1442 6	1874 4	148 08	1284 2	2073 1	161 92	22 803	22 903	23 237
-29 7	1584 3	1901 1	157 37	1416 5	2126 0	172 03	22 770	22 882	23 252
-4 9	1691 0	1927 6	165 96	1535.1	2124 2	179 15	22 763	22 861	23.183
19 8	1778 4	1963 3	174 73	1669 0	2091 0	183.58	22 792	22 836	23.066
44 5	1959 3	1997 3	182 97	1801 4	2172 2	195 17	22 760	22 853	23 132
69 2	2116 7	2021 5	188 87	1899 0	2252 3	203 83	22 743	22 852	23 212
94 0	2290 9	2043 6	194 16	1998 4	2310 6	212 91	22 727	22 852	23 261
118 7	2365 9	2061.0	198 64	2069 4	2356 4	218 56	22 713	22.849	23 296
143 4	2463 0	2075 7	202 27	2134 7	2395 0	224 97	22 703	22 848	23 327
168 2	2510 2	2084 9	204.00	2179 0	2401 0	227 30	22 703	22 847	23 319
192 9	2520.7	2090 7	206 01	2203 1	2392 1	227 61	22 711	22 848	23 298
217 6	2504.9	2091 4	205 77	2200 4	2380 9	226 92	22 719	22 850	23 284
242 4	2455.1	2087 7	204 20	2173 3	2356 2	223 49	22 732	22 854	23 259
267 1	2242 2	2081 3	201 41	2120 4	2290 5	216.36	22 766	22 863	23 183
291 8	2213 0	2070.0	196 36	2056 0	2229 6	208 25	22 801	22 876	23 122
316 6	2074.0	2055.9	190 73	1957 0	2179 5	199 41	22 836	22 895	23 089
341 3	1935 7	2032 0	181 96	1819 7	2161 5	188.84	22 855	22 917	23 123
366 0	1791.5	1992 2	167 91	1610 2	2216 4	182 55	22 848	22 955	23 189
390 7	1673 4	1956 5	161 44	1505 0	2175 3	175 97	22 838	22 945	23 297
415 5	1534 4	1924 5	157 98	1440 9	2049 3	166 12	22 855	22 918	23 126
440 2	1413 0	1889 0	153 55	1372 5	1956 0	157 27	22 888	22 909	23 007
464 9	1274 0	1870 3	145 74	1267 7	1880 6	146 40	22 918	22 924	22 942
489 7	1189 3	1843 3	137 49	1166 2	1832 6	137.02	22 951	22 946	22 926
514 4	1072 0	1811 9	130 22	1072 0	1813 3	130 30	22 956	22 957	22.939
539 1	991 5	1788 1	123.35	992 0	1787 2	123 30	22 979	22 978	22 976
563 9	910 0	1761 6	117 14	919.7	1758 5	116 96	22 992	22 991	22 985
588 6	855 1	1736 9	111 38	854 9	1737 2	111 39	23 004	23 004	23 004
613 3	823 6	1709 0	105 89	793 8	1773 9	109 32	22 974	23 012	23 131
638 1	729 2	1690 9	100 62	743 9	1665 5	90 88	23 070	23 070	22 985

TABLE 2 : SUMMARY OF TESTS

a) Nitrogen

Test No	P_{max} Kg/cm^2	T_{max} K	ρ_{max} (Amagat)
S/R=21.5	Nitrogen		
70	2390	1323	-
73	1960	1390	253
75	1770	1400	235
76	2250	1420	265
77	2580	1420	285
S/R=22	Nitrogen		
78	1220	1450	177
79	1215	1320	174
80	1900	1420	225
81	2560	1435	262
82	2720	1625	245
83	3050	1670	256
84	2385	1440	245
85	2660	1560	242
87	3435	1675	301
S/R=22.4	Nitrogen		
14	1955	1795	204
15	1168	1567	156
20	2394	1830	237
26	1200	1555	157
S/R=22.8	Nitrogen		
5	2240	1960	202
6	733	1600	109
8	1070	1705	136
19	2922	2126	234
S/R=23.1	Nitrogen		
10	1460	1930	154
12	2520	2090	206
21	3116	2275	187
24	2528	2124	203
25	2712	2190	212

Test No	P_{max} Kg/cm^2	T_{max} K	ρ_{max} (Amagat)
S/R=23.5	Nitrogen		
13	3020	2320	220
23	1960	2240	163
184	940	1700	100
185	1580	1970	128
186	2250	2030	166
187	2720	2110	185
188	3060	2165	186
191	455	1460	69
S/R=24	Nitrogen		
192	305	1495	45
193	313	1500	48
195	131	1305	25
196	217	1320	34
197	383	1565	54
198	760	1760	86
199	1410	1790	125
200	1320	1955	122
201	2010	2180	163
202	2120	2095	157
203	2435	2175	178
S/R=24.5	Nitrogen		
204	220	1570	34
205	283	1550	38
206	535	1830	60
207	1075	2150	95
208	1630	2240	124
211	142	1380	24
230	4790	3060	232

S/R=25.	Nitrogen		
Test No	P_{max} Kg/cm^2	T_{max} K	ρ_{max} (Amagat)
212	680	1945	60
213	745	2080	70
214	1045	2280	95
215	1535	2385	105
216	1236	2270	95
217	410	1813	44
218	217	1625	28
220	100	1395	16
231	4460	3255	175
S/R=25.5	Nitrogen		
221	235	1745	25
222	680	1950	54
223	1035	2345	71
224	965	2330	70
233	4150	3450	155

b) Air

S/R=22.	Air		
228	2235	2030	275
S/R=22.5	Air		
88	740	1570	128
89	993	1713	163
90	1055	1745	170
91	1185	1775	181
92	966	1760	162
93	1025	1765	-
94	945	1655	157
95	790	1680	144
96	1665	1665	218

Test No	P_{max} Kg/cm^2	T_{max} K	ρ_{max} (Amagat)
97	1415	1920	195
98	1280	1750	188
99	1765	1900	211
100	2365	1990	252
102	1990	1905	210
103	2990	1985	287
S/R=23.	Air		
112	467	1500	-
113	560	1590	108
114	755	1660	130
115	1200	1770	165
116	1500	1915	185
117	2770	2020	245
118	1420	1935	185
122	370	1575	74
S/R=23.5	Air		
123	785	1710	120
124	830	1775	-
125	855	1750	127
127	1620	2010	180
128	2685	2045	235
129	2845	2045	-
130	3085	2045	245
S/R=24.	Air		
38	1500	2050	155
39	785	1850	105
40	727	1830	100
41	955	2130	120
50	1290	2285	140
51	2510	2120	191
56	1690	2180	165
132	2290	2040	187
133	3230	2020	232
135	355	1605	65
136	340	1620	64

Test No	P_{max} Kg/cm^2	T_{max} K	ρ_{max} (Amagat)
137	575	1550	89
138	870	1710	115
139	450	1630	74
141	202	1680	-
142	390	1420	-
143	330	1620	59
144	210	1410	45
S/R=24.5	Air		
42	420	1870	63
44	680	1980	86
45	1060	2115	113
46	1430	2250	124
48	985	2260	102
147	100	1345	23
153	210	1440	39
154	325	1810	50
155	510	1915	71
156	3335	2235	208
S/R=25.	Air		
157	155	1580	27
158	200	1680	32
159	425	1760	53
160	535	1940	62
161	540	2130	64
S/R=25.5	Air		
163	330	1720	41
164	440	1860	50
165	645	2040	71
166	735	2045	68
167	1065	2200	95
168	925	2130	67
169	920	2180	67
177	285	1780	35
178	120	1600	18

Test No	P_{max} Kg/cm^2	T_{max} K	ρ_{max} (Amagat)
179	123	1720	19
235	4285	3275	250
S/R=26.	Air		
170	445	2055	36
173	645	2090	43
176	433	1950	36
236	4875	3265	165
S/R=26.5	Air		
181	685	2115	36
182	305	2010	24
237	2415	3290	81

LIST OF SYMBOLS

h	Planck constant
H	enthalpy
k	Boltzmann constant
L	displacement of the piston
M	number of moles
P	pressure
R	gas constant
S	entropy
SLR	sodium line reversal
T	temperature
v	voltage
V	volume
ν	frequency
ρ	density
ϕ	diameter

Subscripts

0	reservoir
1	calculated value of entropy using ρ and T
1	emission
2	calculated value of entropy using P and T
2	lamp emission
3	calculated value of entropy using P and ρ

3	absorption
4	barrel
f	final conditions
i	initial conditions
L	lamp
s	sodium atoms